TRACE METAL DISTRIBUTION IN REDEPOSITED ORGANIC CARBON-RICH SEDIMENTS IN A MODERN UPWELLING SYSTEM

By

DOUGLAS W. ASHE

Bachelor of Science in Geology

Oklahoma State University

Stillwater, OK

2016

Submitted to the Faculty of the
Graduate College of the
Oklahoma State University
in partial fulfillment of
the requirements for
the Degree of
MASTER OF SCIENCE
July, 2018

TRACE METAL DISTRIBUTION IN REDEPOSITED ORGANIC CARBON-RICH SEDIMENTS IN A MODERN UPWELLING SYSTEM

Thesis Approved:

Dr. Natascha Riedinger

Thesis Adviser

Dr. Javier Vilcaez-Perez

Dr. G. Michael Grammer

ACKNOWLEDGEMENTS

I would like to thank my adviser, Dr. Natascha Riedinger for her patience and help in the lab and in the process of writing this thesis. It would have been impossible without her help. I would also like to thank my committee members, Dr. Javier Vilcaez-Perez and Dr. G. Michael Grammer, for their advice and help with this project. I would also like to thank Michelle Abshire for her help with editing and in the lab. Thanks to the Boone Pickens School of Geology for allowing me, and funding me to do this project.

Name: DOUGLAS W. ASHE

Date of Degree: JULY, 2018

Title of Study: TRACE METAL DISTRIBUTION IN REDEPOSITED ORGANIC CARBON-RICH SEDIMENTS IN A MODERN UPWELLING SYSTEM

Major Field: GEOLOGY

Abstract:

To determine the depositional pathways and environments of organic carbon-rich material, sediment cores from the Benguela upwelling system offshore Namibia were investigated. Trace and major elements, organic carbon, and calcium carbonate were analyzed in sediments from three cores collected on the upper, middle, and lower continental slope. The results show that decoupled cadmium and zinc profiles as well as silver depletions in these sediments around the last glacial maximum suggest a change in the nutrient source in upwelled waters which may have impacted primary productivity. Vanadium accumulation correlates strongly with nickel and TOC accumulation in sediments on the lower and middle continental slope. This correlation is lost in sediments higher on the slope. The lack of correlation between nickel and vanadium with TOC in the upper slope core indicates redeposition of reworked, laterally transported sediments from the continental shelf. Additionally, at all three core sites, vanadium shows strong correlation with iron and manganese, indicating that oxic bottom waters have been present during much of the recorded time period. The proxies evaluated in this study suggest that during the last glacial maximum in the Benguela upwelling system around our study sites, intensified upwelling incorporated nutrients from a different source. An increase in primary productivity around that time period resulted in increased deposition of organic carbon-rich materials on the continental slope.

TABLE OF CONTENTS

Chapter Page

LIST OF TABLES

Table Page

LIST OF FIGURES

Figure Page

CHAPTER I

INTRODUCTION

Coastal upwelling of nutrient-rich, cool waters results in high primary productivity and, consequently, in the potential accumulation of organic matter (e.g., Berger and Wefer, 2002; Summerhayes et al., 1995; Hutchings et al., 2009). These processes have been observed in the Benguela upwelling system (Inthorn et al., 2006; Zabel et al., 2003; Mollenhauer et al., 2002). Three cores from the continental slope have been examined to determine the impact of processes such as eustatic changes, upwelling intensity, and changing redox environment on trace metal distribution in organic carbon-rich sediments.

Benguela Upwelling System

The Benguela upwelling system offshore Namibia, southwest Africa (between 17ºS and 37ºS; Figure 1), is one of the most important upwelling regions in the modern ocean, with intense primary productivity leading to elevated deposition of organic carbon (Embley et al., 1980; Robinson et al., 2002; Inthorn et al., 2006a). Perennial upwelling of nutrient-rich waters responsible for high primary productivity results in significant accumulation of organic-rich sediments on the continental shelf (e.g., Carr, 2001; Marchesiello et al., 2009).

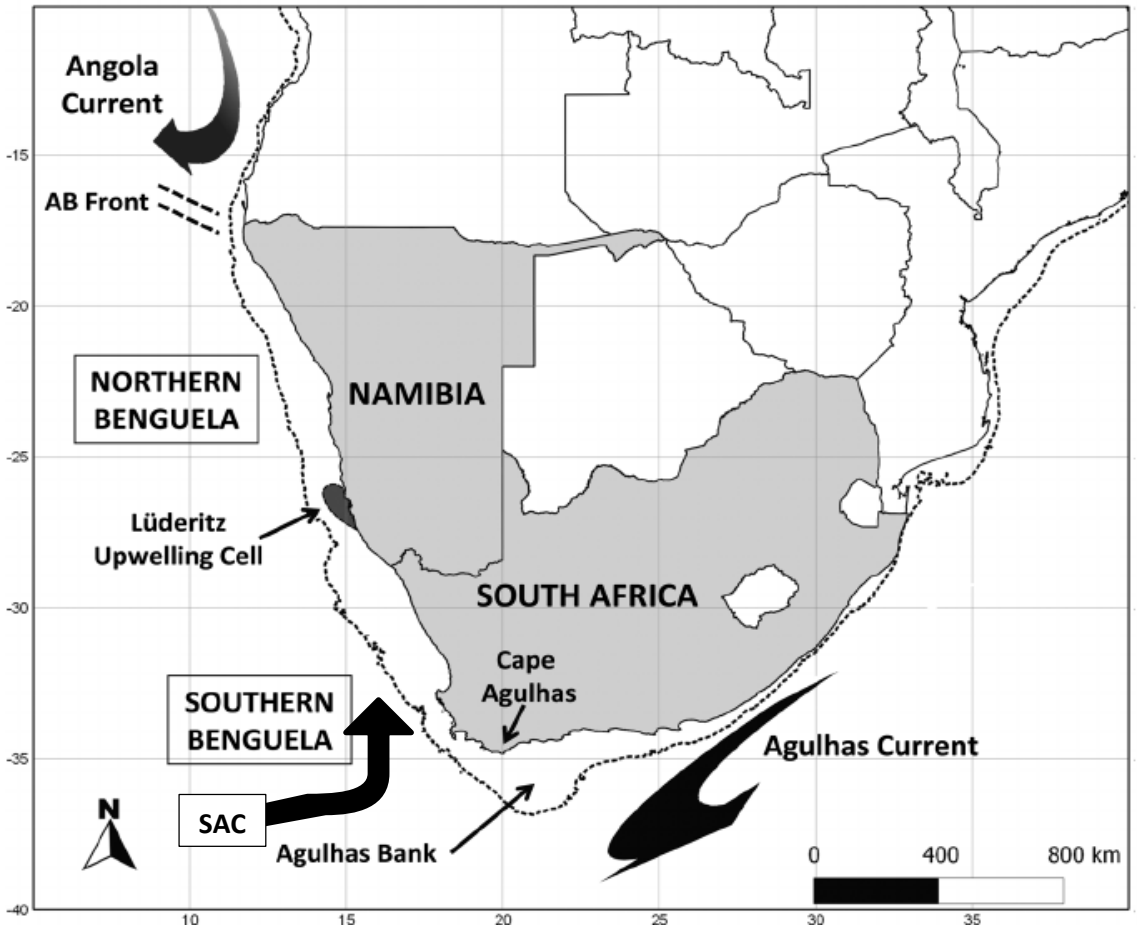

Figure 1. Map of the Study Area. Locations of the Angola current, South Atlantic current (SAC), Agulhas current, and Lüderitz upwelling cell which separates the northern Benguela upwelling from the southern Benguela upwelling. The approximate location of the Angola-Benguela Front is indicated by strong dashed lines, and the weak dashed line indicates the 500-m bathymetric contour (modified from Roux et al., 2013).

Upwelling occurs as Ekman transport deflects northward flowing Benguela coastal current (BCC) surface waters - driven by winds blowing from the southeast and

parallel to the shoreline (Figure 2) - to the west in a system of incrementally deflected water layers with increasing depth. The result is an overall northwesterly subsurface flow (Volbers et al., 2004). The displacement of surface water is then replaced by upwelled cold and nutrient-rich water (Volbers et al., 2004; Berger et al., 2002; Boyer et al., 2000), sourced from the South Atlantic Central Water (SACW) (Shannon, 1985; Volbers et al., 2004; Giraudeau et al., 1994; Inthorn, et al., 2006b). These nutrient-rich waters are upwelled from beneath the thermocline—the zone where warm surface waters rapidly decline in temperature over a short distance—at about 50-200 m water depths in this particular region (Inthorn et al., 2006b; Allaby, 2008). At that depth, the nutrient-rich SACW, containing dissolved oxygen of approximately 4.8-5.2 mL/L (80-85% saturation), is entrained in a south poleward flowing current, which overlies the colder, northward flowing Antarctic Intermediate Water (AAIW) (Inthorn, et al., 2006b; Stramma, et al., 1999; Des Combes and Abelmann, 2007). Peak upwelling intensity occurs perennially at Lüderitz (27°S-28°S) (Boyer et al., 2000; Shannon, 1985), just south of the study area. At this location, the Benguela Current (BC) diverges into the westward flowing Benguela Oceanic Current (BOC) and the northward flowing Benguela Coastal Current (BOC) (Figure 2) (Stramma et al., 1989; Boyer et al., 2000). The Lüderitz upwelling cell extends cold (approximately 16ºC), nutrient-rich water seaward approximately 270 km from the coast on average, and is considered the upwelling center of the system (Lutjeharms et al., 1987).

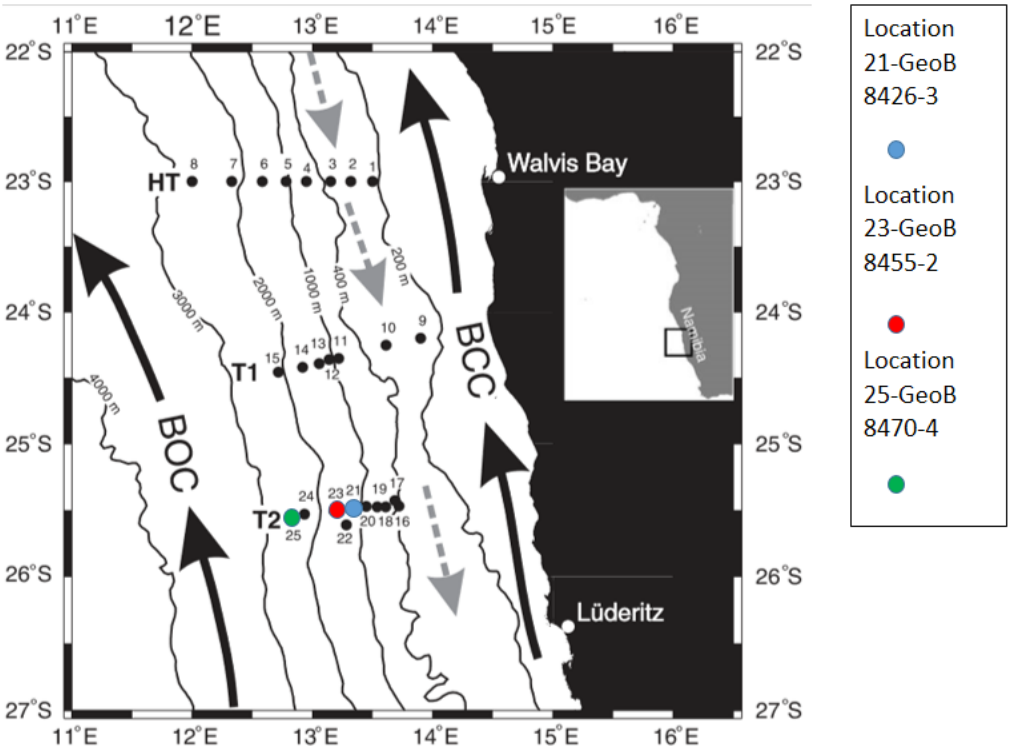

Figure 2. Location of Cores. Bathymetry of the Namibian continental margin and location of gravity cores collected during expedition M57/2 onboard the RV *Meteor* at GeoB stations along transect 2 (T2). Other transects shown. The Benguela current segments are indicated by black arrows: Benguela Oceanic Current (BOC) and Benguela Coastal Current (BCC). Gray arrows indicate flow of the South Atlantic Central Water. Modified from Inthorn et al. (2006)

Wind strength and direction variability impact the intensity of upwelling both temporally and spatially (Stramma et al., 1989). An extensive mixing area extends more than 600 km seaward, where nutrient-laden filaments (surficial current-mobilized nutrient patches which extend upwelled particle content seaward above the continental slope) can

impact productivity (Lutjeharms et al., 1987; Inthorn et al., 2006b). In total, the extent of upwelling impact can be up to 1000 km from the coast (Lutjeharms et al., 1991). Upwelling that occurred during the last glacial maximum (LGM) may have been more powerful than contemporary upwelling due to intensification of trade winds during this period (Sarnthein et al., 1988).

Productivity and Sediment Deposition

Because upwelled SACW waters are nutrient-rich, they support high levels of primary productivity (Carr 2001). Cold-water plankton assemblages take advantage of these nutrients, generating a zone of high productivity in the surface water (Volbers et al., 2004; Gingele et al., 1994; Embley et al., 1980). High productivity parallel to the Namibian coastline has led to high accumulation of total organic carbon (TOC) in surface sediments - primarily in three regions: on the Walvis Plateau, near Walvis Bay, and north of Lüderitz (Mollenhauer et al., 2002; Inthorn et al. 2006a, 2006b). These regions of high TOC content in surface sediment are derived from a diatomaceous mud belt, which is the shelf depocenter for productivity in the modern Benguela system. (Bremner, 1980).

Modern sediment flux into this system is primarily biogenic. Major biogenic components include diatoms, foraminifera and dinoflagellates (Hansen et al., 2014; Des Combes and Abelmann, 2007; Mollenhauer et al., 2002). Low terrigenous input from perennial fluvial sources such as the Orange River, can be transported northward to the study area as sediment load within the Benguela Current (Bremner et al., 1993; Diester-

Haass et al., 1988). Data from a downslope transect around 23°S in the Cape Basin indicate that the lysocline in this area is below 4100 m water depth with a calcite saturation horizon near 3900 m water depth (Dittert and Henrich, 2000). Good preservation of calcium carbonate in water above ~3900 m and minimal riverine sediment flux beyond the continental shelf result in continental slope deposits primarily composed of calcareous ooze (Bremner et al., 1993; Rogers et al., 1991; Inthorn et al., 2006b). During cooler periods such as the last glacial maximum (LGM) intermittent streams like the Swakop River may have had an increased impact on sedimentation, as suggested by slight increases in terrigenous matter from the Namib Desert (Diester-Haass et al., 1988).

Shelf mudbelt deposits account for about 85% of TOC accumulation in the modern setting off Namibia (Mollenhauer et al., 2002). However, during the last glacial maximum, the location of highest deposition of TOC migrated seaward, relative to the modern depocenter (Mollenhauer at al., 2002). The contemporary continental shelf offshore southwest Africa is characterized by a deep and wide water column (Mollenhauer et al., 2002). During the LGM, the water column may have been too shallow for an upwelling system to develop; the upwelling system likely migrated westward, thereby dislocating organic-rich depocenters as much as 10-110 km offshore (Mollenhauer et al., 2002). Additionally, reworking and redistribution of shelf sediments to the slope occurs in subsurface currents in the modern system (Inthorn et al., 2006a, 2006b), and also likely occurred during the LGM (Summerhayes et al., 1995; Robinson et

al., 2002; Inthorn et al., 2006a, 2006b). The greatest displacement of the organic matter depocenter has occurred during sea level lowstands, placing the center seaward of the current location (Summerhayes et al., 1995; Mollenhauer et al., 2002).

Formation of the Oxygen Minimum Zone

The degree of organic matter remineralization is related to the availability of oxygen in the water column and has been regarded as one of the determining factors for OM preservation in marine sediments (Demaison et al., 1980). Oxygen in the water column is consumed at the surface by respiration (Borchers et al., 2005; Capone et al., 2013), and further depleted in the water column by microbial degradation of organic matter (e.g. Hensen et al., 2006). This process occurs as nutrient upwelling stimulates growth of phytoplankton at the top of the water column in the photic zone, followed by export of sinking organic carbon-rich particulates (Suess et al., 1983; Summerhayes et al., 1995). As particulate organic matter (POM) settles out of the water column, remineralization – POM degradation or dissolution of hard parts leading to the solubilization of nutrients and micronutrients – drives the consumption of dissolved oxygen, thereby generating an oxygen-depleted water mass known as an oxygen minimum zone (OMZ) (Pederson et al., 1990; Bailey, 1991; Rullkötter, 2006; Inthorn et al., 2006b). On continental margins, the OMZ may extend down to the sediment-water interface (Rullkötter, 2006). The modern OMZ offshore Namibia is found in water depths between 150 and 450 meters (Figure 3) (Bailey G. , 1991). Beneath the OMZ, abundant

free oxygen is replenished by circulation of deep currents (Stramma et al., 1999). Vertical mixing of oxic bottom waters and waters of the OMZ is inhibited by thermocline density stratification (Borchers et al., 2005; Chapman et al., 1985).

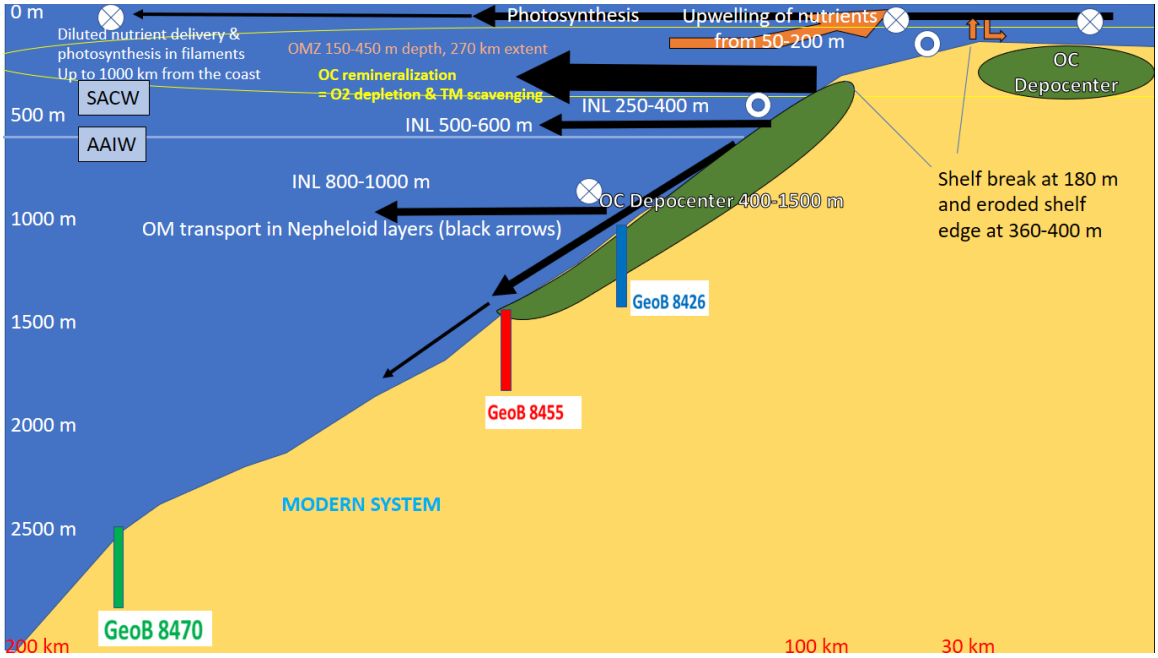

Figure 3. Modern Benguela Upwelling System. White rings indicate poleward flowing currents, and circles with an X indicate equatorward flowing currents. Black metrics represent water column depth and red metrics indicate distance from shore (figure is not to scale). Inset modified from Inthorn et al., 2006. SACW = South Atlantic Central Water; AAIW = Antarctic Intermediate Water

Preservation of Organic Matter

Only a small proportion of the primary production generated in the photic zone is incorporated into the geologic record partly due to the array of biological and chemical processes taking place in the water column during particle settling (Wakeham et al., 1989; Emerson et al., 1988). Depending on factors such as water depth, abundance of primary productivity, particle size, adsorption to mineral surfaces and sediment porosity, the proportion of primary production of organic matter that is ultimately preserved is between 1 and 0.01% (Rullkötter, 2006). These numbers are representative of organic matter accumulation in an oxic water column; whereas in an anoxic depositional setting, possibly 2% or more of the primary production of organic carbon is preserved in benthic sediments (Rullkötter, 2006; Bralower et al., 1987). Anoxic environments, in contrast to settings with abundant free oxygen in the water column, are characterized by relatively lower intensity of OM degradation, thereby creating settings favorable for the preservation of sediments rich in organic carbon (Rullkötter, 2006).

Sediment Transport and Redeposition of Organic Material

Sediment reworking and relocation can have an additional impact on TOC signals in this system, and lateral particle transport within nepheloid layers has been considered the primary means of organic-rich sediment supply and burial on the continental slope in Benguela upwelling system (Inthorn et al., 2006a, b; Mollenhauer et al., 2007). Impacted by the previously described currents, nepheloid layers are layers of water with relatively

higher particle content than surrounding water that occur in a variety of locations within the Benguela upwelling system (Inthorn et al., 2006b). Three general types of nepheloid layers were observed in the water column above the cores used in this study: surface nepheloid layers (SNL), intermediate nepheloid layers (INL) and bottom nepheloid layers (BNL; Figure 3) (Inthorn et al., 2006b). They can range from several to hundreds of meters in thickness, and the intensity of BNL sediments decreases with distance from shore along the core transect used in this study (Inthorn et al., 2006b). Both intermediate and bottom nepheloid layers are important long-distance vehicles for the lateral transportation of shelf sediments to the slope and deep sea (Jahnke et al., 1990). High sedimentation rates of organic-rich material on the Namibian continental slope have been attributed to transport in the BNL, originating from the shelf break (Inthorn et al., 2006a) at around 360-400 meters' water depth off the coast of Namibia (Zabel et al., 2003; Inthorn et al., 2006b).

In the Benguela upwelling system, periods of eustatic change may heavily influence OM deposition in deep water environments by catalyzing remobilization and lateral transport of shelf sediments rich in organic matter (Inthorn et al., 2006a).

Trace Metal Geochemistry

In order to identify variations in depositional pathways, depositional environments, and diagenetic alterations during burial of organic carbon-rich material in the Benguela upwelling system, trace metals have been analyzed in the three cores used

for this study. Trace metals are supplied to the marine sediment through biogenic uptake processes and incorporation into cellular organic carbon, adsorption to surfaces of iron and manganese oxides and particulate organic carbon as the sediments fall through the water column, or as terrigenous input (Balistrieri et al., 1981; Diester-Haass et al., 1988; Little et al., 2015). In upwelling systems, accumulation of TOC is enhanced due to high organic particle flux as well as intensified preservation of organic carbon-rich sediments in the water column (Demaison and Moore, 1980; Böning et al., 2015) - processes which can be identified using trace metal proxies.

Trace metals are useful as redox indicators in the sediment column because many are enriched under euxinic, organic-rich conditions, and poorly enriched if at all in organic-poor deposits (e.g., Calvert and Pedersen, 1993; Algeo et al., 2004; Algeo and Lyons, 2006;). For example, molybdenum (Mo) and uranium (U) are covariant with organic carbon contents during depositional and burial processes under euxinic (anoxic with sulfidic) water column conditions (e.g., Bertine, 1972; Emerson and Huested, 1991; Calvert and Pedersen, 1993; Algeo et al., 2006; McManus et al., 2006; Scott et al., 2013). Many trace metals such as cadmium, nickel, silver and vanadium make useful productivity indicators because they are essential as physical components and reactive centers of metalloenzymes in marine organisms (Robbins et al., 2016; Cole et al., 2017; Georgiev et al., 2015; Dupont et al., 2010; Crusius and Thomson, 2003). Therefore, productivity of phytoplankton is significantly affected by the availability of biolimiting

trace metals (such as cadmium, nickel, silver and vanadium) in seawater (Martin et al., 1988).

Some major metals can have similar importance as productivity and redox indicators. Iron (a major metal) is both bioessential and redox-sensitive. It can be introduced into the water column as oxide/hydroxide coatings on terrigenously sourced mineral grains, especially during glacial periods when intensified trade winds transport sediments from the Namib desert to the water column (Borchers et al., 2005; Diester-Haas et al., 1988). As an important limiting element, it is used as a cellular component of some organisms (Morel et al., 1991). In oxic water, iron (III) forms low solubility iron oxyhydroxides (Millero et al., 1987), and is highly reactive in the presence of sulfides in a euxinic water column (Yao and Millero, 1987; Borchers et al., 2005; Boyd et al., 2007).

Cadmium (Cd)

The distribution of cadmium in seawater can be correlated to its use as a biologic component (Abouchami et al., 2011). Plankton can accumulate cadmium in concentrations two orders of magnitude greater than the terrigenous detrital fraction (Heinrichs et al., 1980; Brumsack, 2006). Cadmium can substitute for zinc in an enzyme called carbonic anhydrase used by diatoms for the photosynthetic acquisition of inorganic carbon (Price et al., 1990). The final accumulation of cadmium in the sediment column is related to the produced sulfide, which makes Cd an indicator of redox conditions as well as productivity (Böning et al., 2004; Rosenthal et al., 1995).

Nickel (Ni)

Due to excellent correlation between nickel and TOC in a Peruvian upwelling sediment column, it is argued that the main water column removal mechanism for Ni in that location is association with organic matter (Böning et al., 2015). A similar trend in sediment columns off the coast of Namibia has been observed, with lower r^2 values due to dilution with opal (Böning et al., 2015). Other authors concur with the observation that nickel plays a biological role, as is evidenced by behaviors similar to phosphate and silica (major biogenic components) seen in water column profiles (Dupont et al., 2010; Price et al., 1990; Morel et al., 1991; Tribovillard et al., 2006).

Silver (Ag)

Silver can be used as a proxy for flux of diatoms to the seafloor (Crusius et al., 2003). Water column profiles for silver typically show a strong depletion of the metal at the sea surface where Ag is removed by organisms for metabolic use. As their bodies die and fall through the water column, they are remineralized causing steady Ag release into the water column with increasing depth (Martin et al., 1983). Correlation between water column profiles for Ag and Si could indicate that Ag is incorporated into the tests of diatoms before being partly transported through the water column (Flegal et al., 1995). Experiments have made it clear that (siliceous) diatoms have a much higher affinity for Ag than coccolithophoridae, which build carbonaceous tests (Fisher et al., 1993). Another mechanism of Ag transport to the sea floor is particulate scavenging (McKay et al.,

2000). A likely mechanism for Ag sequestering in the sediment column is immobilization by sulfide in bottom water, and deposition of Ag_2S, making silver yet another indicator of redox conditions (Rosenthal et al., 1995).

Vanadium (V)

Vanadium can be utilized as an indicator of euxinic or anoxic redox conditions in the sediment column based on levels of enrichment (Algeo et al., 2004; Scott and Lyons, 2012). The vanadate anion ($H_2VO_4^-$) is stable in oxygenated waters, where it adsorbs to iron oxyhydroxides (Wehrli et al., 1989). Under anoxic conditions, V (V) is reduced to the vanadyl ion ($V(IV)O^{2+}$), a smaller cation which adsorbs to organic particles even more readily than the vanadate anion does. Vanadium (IV) can further be reduced to V(III) under conditions where H_2S is present (Borchers et al., 2005; Wanty et al., 1992). While bioessential trace metals like silver, cadmium, and nickel are pre-concentrated by biological processes prior to burial, oxyanions containing vanadium enrich marine sediments according to their availability in seawater. Vanadium can, however, show intermediate behavior with some sediment enrichment ascribed to biological pre-concentration (Borchers et al., 2005; Hatfield et al., 1991).

CHAPTER II

MATERIALS AND METHODS

Gravity cores GeoB 8426-3, GeoB 8455-2 and GeoB 8470-4 were collected during the RV *Meteor* expedition M57/2 in the eastern South Atlantic on the continental margin off Namibia (see Figure 2). The area of our study in this system is near 25°S latitude, south of the Walvis Bay upwelling cell (near 23°S latitude) and north of the strong perennial Lüderitz upwelling cell (Inthorn et al., 2006b) at about 26.5°S. Core data retrieved from Zabel et al. (2003) are shown in Table 1. The scientific investigations completed during the cruise of the RV *Meteor* are described in detail by Zabel et al. (2003).

Table 1. Names, locations and water depths of cores used in this study

Core	Latitude	Longitude	Water Depth (m)
GeoB 8426-3	25°28.9 S	13°21.1 E	1045
GeoB 8455-2	25°30.4 S	13°11.0 E	1502
GeoB 8470-4	25°32.7 S	12°51.6 E	2470

The modern accumulation rates of sediments in the cores utilized for our study (on the continental slope) have been estimated to have an average of 8-10 cm/ka in core GeoB 8470, and 16-20 cm/ka in cores GeoB 8426 and GeoB 8455, using correlation of geophysical signals to observed profile of marine isotope stages in this area. (Zabel et al., 2003).

Trace metal analysis was performed in the Riedinger lab at Oklahoma State University in Stillwater, Oklahoma. Samples from 3 cores totaling 149 samples, 5 blanks, and 5 reference material (NIST 2702) samples were processed. Approximately 100 mg of each sample was ashed at 550°C for 10 hours in a Thermo Fischer Scientific Furnace. A multi-acid digestion procedure using 3 mL nitric acid, 3 mL hydrochloric acid, and 2mL hydrofluoric acid was carried out. Samples were heated on a PicoTrace© Pressure Digestion System heating block for approximately 12 hours for total digestion. They were moved to an evaporation apparatus using the same system for 10 ½ hours to evaporate all liquids. Dried samples were taken up in 10 mL of a 5% nitric acid solution. For this study, a Thermo Fisher Scientific iCAP Q© Inductively Coupled Plasma-Mass Spectrometer in the Riedinger lab at Oklahoma State University was utilized for elemental composition analysis. Total carbon and total organic carbon (TOC) contents were determined using a LECO CS-300 carbon sulfur analyzer (for details see Riedinger et al., 2006). Inorganic carbon was determined by subtracting TOC from total carbon in each sample. Calcium carbonate was calculated (assuming that other carbonate phases can be neglected) using the formula: $(Total\ carbon - TOC) * 8.33 = CaCO_3$.

CHAPTER III

RESULTS

Sediment Color Scans

Color scans of cores used in this study and parallel cores (Appendices A, B, and C) have been retrieved from Zabel et al. (2003) and used for comparison with TOC and $CaCO_3$ profiles. Darker-colored beds generally correspond to TOC enrichments in core profiles while lighter-colored beds correspond well with $CaCO_3$ enrichments and TOC depletions, as seen in enhanced images of each of the cores (Fig. 4). The enhanced image of core GeoB 8426-3 is similar to the enhanced image of nearby core GeoB 8426-2 (Fig. 4). Because no lithologic profile could be found for core GeoB 8426-3, the lithology of parallel core GeoB 8426-2 will be used for context. The lithologic profile of core GeoB 8426-2 is characterized by olive gray to dark olive gray nannofossil and foram oozes (dominating above 7 m depth) with diatom oozes (dominating below 7 m depth). At around 1-3 m and 4-6 m clays form a constituent. Similar to the situation described above, core GeoB 8455-2 has an enhanced image available (Fig. 4) but not a lithologic profile. There is a lithologic profile available for a parallel core (GeoB 8455-3) that was collected nearby core GeoB 8455-2. Core GeoB 8455-3 is characterized by intercalated olive gray, dark olive gray, and dark gray beds. Foram-nannofossil ooze is prevalent in the surficial sediments, grading into nannofossil, foram, and clay-bearing diatom oozes.

The deepest section of the core (from about 9.5 m to the bottom) is a clayey-diatom-bearing foram-nannofossil ooze.

A lithologic profile is not available for core GeoB 8470-4. However, an enhanced image of parallel core shows lighter-colored sediments in the top 1 meter and bottom ½ meter of the core. In general, this core has noticeably higher density of darker laminations than the other two cores.

Organic and Inorganic Carbon

The organic carbon content of continental slope sediments (Fig. 4) in core GeoB 8426-3 range from 5.95-11.91 wt. %, 4.8-8.9 wt. % in core GeoB 8455-2, and 1.7-7.7 wt. % in core GeoB 8470. In general, there is a strong decoupling of calcium carbonate from TOC in all cores, with the exception of core GeoB 8455-2 at depths from approximately 4-7 m. The highest content of organic carbon occurs near 6 m sediment depth in core GeoB 8426-3, 3.5 m in core GeoB 8455-2, and at approximately 4 m, 9 m, and 10 m in core GeoB 8470-4. Overall trends in each core show increase in TOC content downcore to the noted locations of enrichment, then generally show a decreasing downcore trend. In contrast to the organic carbon trends in each core, depletions in $CaCO_3$ consistently occur at core depths where enrichments in TOC also occur (for example, 4, 9, and 10 m depth in core 8470), with some exceptions (e.g., at about 4.5 to 7 m in core GeoB 8455-2) (Fig. 4). Calcium carbonates have the highest concentrations near the surface in each of the cores. Near the top of core GeoB 8426-3, the $CaCO_3$ content is greater than 70 wt. %,

just under 70 wt. % near the sediment surface in GeoB 8455-2, and 77.2 wt. % at the top of GeoB 8470-4.

Major Elements (Fe, Al)

Average aluminum content (Fig. 4) in core GeoB 8426-3 is 3.28 wt. %. A notable spike to nearly 5.3 wt. % occurs at approximately 6 m depth. A strong depletion in Al occurs at 6 m depth in both of the other cores. Average Al content in core GeoB 8455-2 is 2.49 wt. %, and 2.12 wt. % in GeoB 8470-4. Both cores, GeoB 8455-2 and GeoB 8470-4, show strong enrichment-depletion cycles on the order of two meters to a half-meter scale overall. Sharp aluminum enrichments and depletions are clearly coupled to iron contents (Fig. 4) in cores GeoB 8426-3 and GeoB 8455-2 in most sections of their profiles, while GeoB 8470-4 aluminum contents are less strongly correlated to Fe. Aluminum and iron contents are relatively depleted at the surface of the sediment column in each core, which correlates to a relative depletion of TOC and enrichment of $CaCO_3$ in all cores. Aluminum and iron profiles for GeoB 8426-3 trend fairly near to their average content with the exception of the previously mentioned depletion near the surface. Profiles of aluminum and iron have stronger variability in enrichment/depletion cycles in GeoB 8455-2 and much stronger variability in enrichment/depletion cycles in core GeoB 8470-4, though the profiles do not correlate with each other. Aluminum and iron profiles contain an enrichment spike just below two meters' depth in all cores.

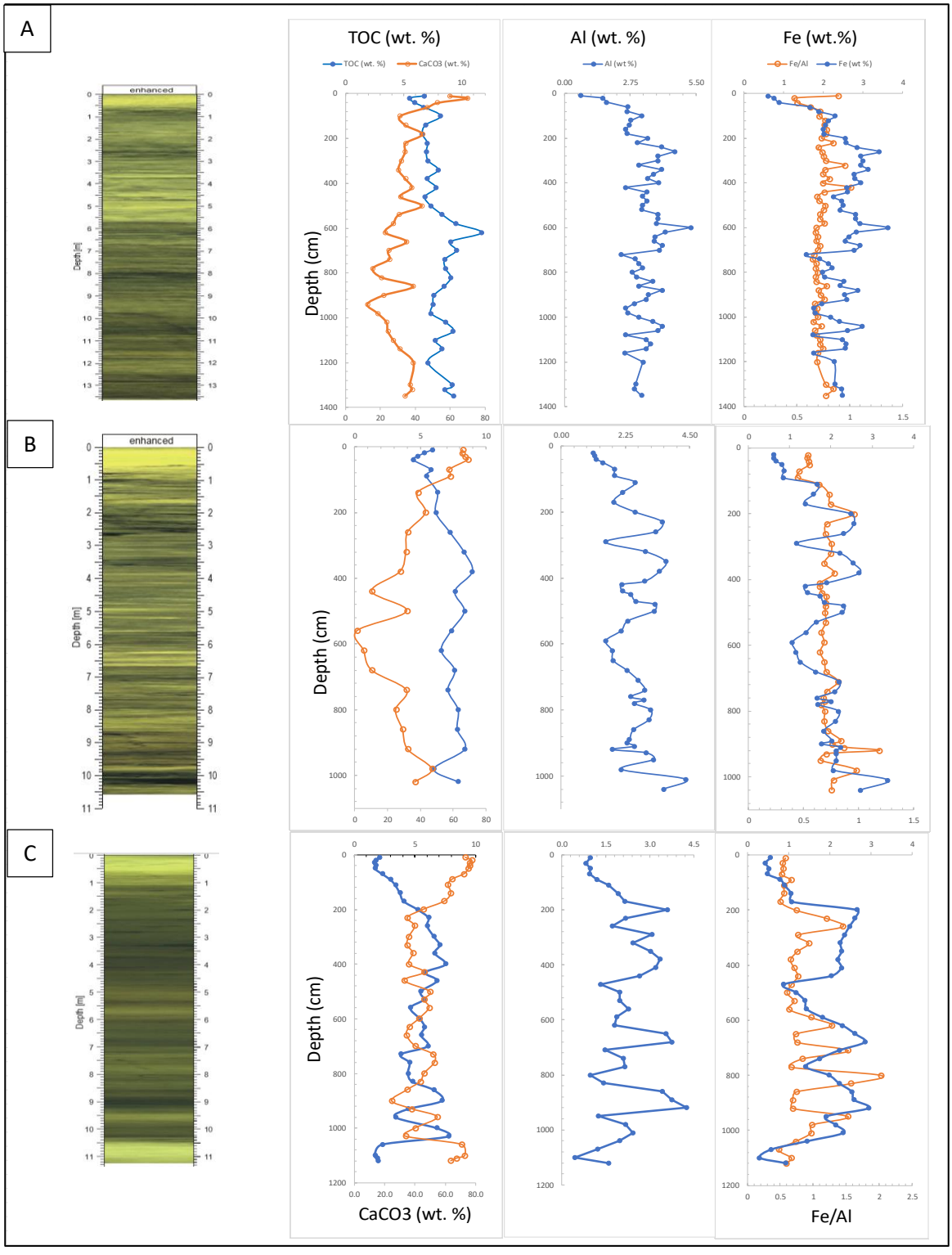
A
B
C
enhanced
Depth [m]
TOC (wt. %)
CaCO3 (wt. %)
Al (wt.%)
Al (wt %)
Fe (wt.%)
Fe/Al
Fe (wt %)
Depth (cm)
CaCO3 (wt. %)
Fe/Al

Figure 4. (Previous page) Color Scans, TOC, $CaCO_3$, Al, and Fe Profiles. Color scans of cores 8426 (A), 8455 (B) and 8470 (C) corresponding to plots of total organic carbon (TOC) plotted with calcium carbonate ($CaCO_3$), Aluminum (Al), and Iron (Fe) plotted with Fe/Al. All profiles plotted against depth (cm). Color scans taken from Zabel et al. (2003).

Trace Metals

Cadmium contents significantly decrease downslope with averages of 5.49 ppm in core GeoB 8426, 3.21 ppm in core GeoB 8455, and 0.72 ppm in core GeoB 8470 (Fig. 5). Cadmium profiles look very similar in all cores, with a small enrichment at 4 meters in core GeoB 8426 and large enrichment near 4 meters in cores GeoB 8455 and GeoB 8470. Cd/Al profiles correlate with Cd versus depth profiles in cores GeoB 8426 and GeoB 8455, with a moderate correlation in core GeoB 8470.

Average nickel contents decrease (Fig. 5), while variability in nickel contents increase downslope from core GeoB 8426 (average 83.3 ppm, range from 55.9-107.3 ppm) to core GeoB 8455 (average 77.3 ppm, range from 44.7-124 ppm) to core GeoB 8470 (average 69.9 ppm, range from 14.9-104.5 ppm).

Average vanadium contents (Fig. 5) are similar in all cores: 66.3 ppm in GeoB 8426-3, 50.5 ppm in GeoB 8455-2, and 49.9 ppm in GeoB 8470-4. Vanadium contents strongly correlate with aluminum and iron contents in core GeoB 8426-3 and more closely to Fe than Al in core GeoB 8455-2.

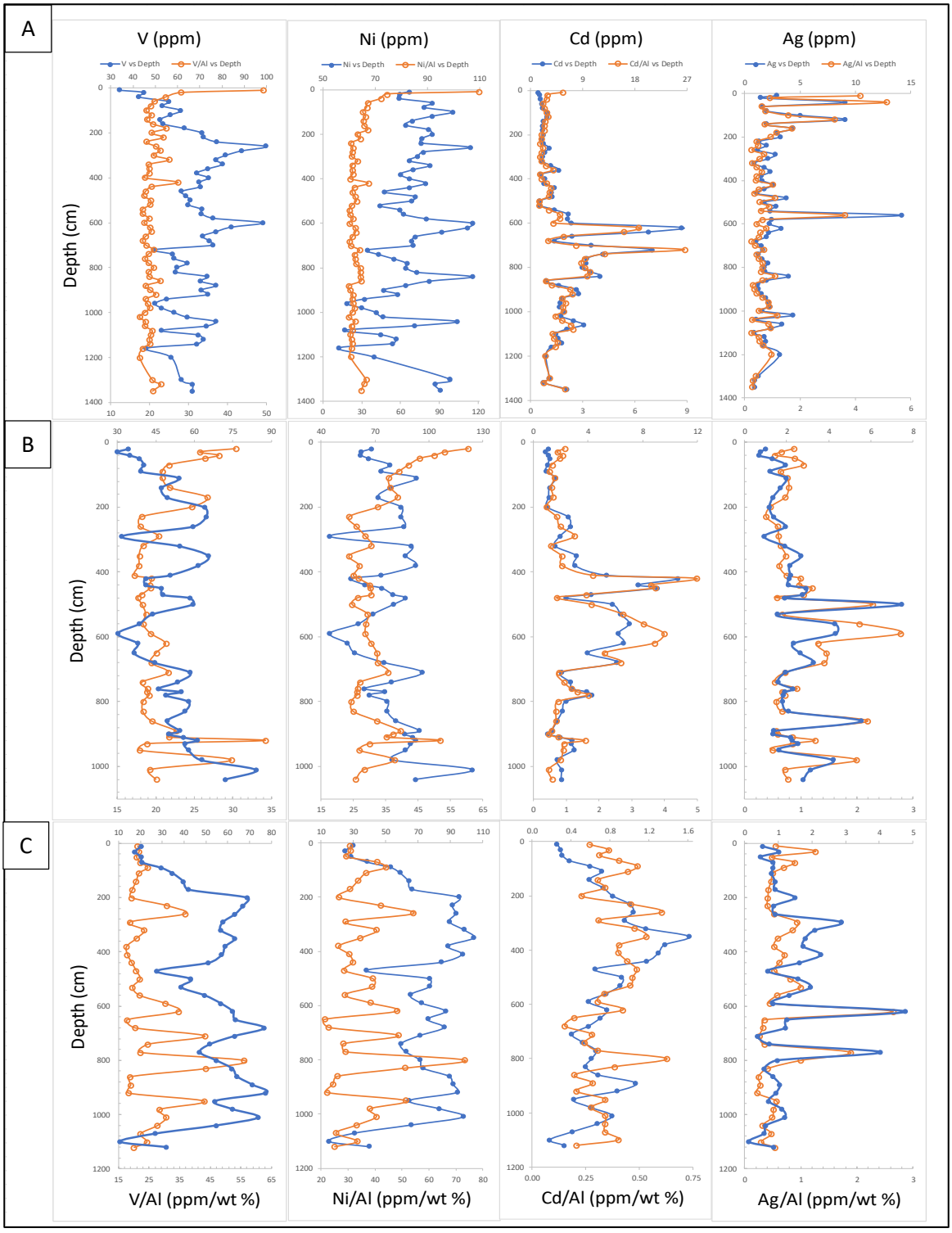
A
V (ppm)
V vs Depth
V/Al vs Depth
Ni (ppm)
Ni vs Depth
Ni/Al vs Depth
Cd (ppm)
Cd vs Depth
Cd/Al vs Depth
Ag (ppm)
Ag vs Depth
Ag/Al vs Depth
Depth (cm)
B
Depth (cm)
C
Depth (cm)
V/Al (ppm/wt %)
Ni/Al (ppm/wt %)
Cd/Al (ppm/wt %)
Ag/Al (ppm/wt %)

Figure 5. (Previous page) V, Ni, Cd, and Ag Profiles. Trace metal profiles for cores GeoB 8426-3 (A), GeoB 8455-2 (B), and GeoB 8470-4 (C). Vanadium (V), nickel (Ni), cadmium (Cd), and silver (Ag) are plotted along with V/Al, Ni/Al, Cd/Al, and Ag/Al profiles (respectively) for normalization against the lithogenic background.

In core GeoB 8470-4, V correlates well with iron. A strong similarity occurs in GeoB 8470-4 profiles of Fe/Al, V/Al, Ni/Al, Cd/Al, and to a lesser degree in Ag/Al.

The silver profile in core GeoB 8426-3 (Fig. 5) shows contents that remain near the average content of 2.5 ppm except at a few very high enrichment spikes within the first two meters (up to 9.09 ppm) of sediment and at 5.6 meters' depth (14.2 ppm). In this core, the Ag/Al ratio remains stable except at the locations with the strongest enrichments. In core GeoB 8455-2, the average silver concentration is 2.3, however this profile has far more variability than core GeoB 8426-3. Sharp enrichment spikes occur near 5 m, 6 m, 8.5 m and 10 m (up to 7.45 ppm). The silver profile for core GeoB 8470-4 shows enrichments near 3 m, 4 m, 6 m, and 8 m (up to 4.8 ppm). This core has an average Ag content of 1.26 ppm.

CHAPTER IV

DISCUSSION

Cores GeoB 8426-3 and GeoB 8455-2 were collected from an organic-rich depocenter (Figure 3) on the upper continental slope, as is reflected in their high TOC content. The observed organic matter enrichment in these cores is in good agreement with findings from previous studies in the Benguela system (Inthorn et al., 2006a; Mollenhauer et al., 2002; Wefer et al., 1998). Core GeoB 8470-4 was collected from the lower slope (outside the TOC depocenter) and has a more variable content profile, yet the overall high average TOC content of 5 wt. % in this core is still remarkable, because the water column above this site is currently oxic. In each of the sediment cores analyzed in this study, TOC exhibits peaks of depletion and enrichment which represent temporal changes in the quantity of organic matter deposition (Figure 4). The top portions of the sediment profiles where modern depositional processes are recorded show that TOC is generally lower than the average contents for each core. This may indicate that the rate of deposition of organic matter has decreased in the recent past as the planet has transitioned from a glacial to an interglacial period.

The TOC and $CaCO_3$ enrichments and depletions (Figure 6) are of paramount importance to this study because they directly correlate to changes in paleoproductivity, and can be used to understand the contribution of sediments to the depositional system

during glacial and interglacial periods. The Namibian shoreline migrated seawards during glacial periods such as the last glacial maximum when sea level fell. Productivity cells at the sea surface moved further out over the continental slope than during oceanic high stands (Mollenhauer et al., 2002). Increased deposition of organic carbon-rich materials occurred further out on the slope during the last glacial maximum, as is reflected in each of the TOC profiles (Figure 6). Each of the core sites record depletions of calcium carbonate in sediments older than the LGM sharply increasing in younger sediments. Organic matter is enriched prior to the LGM, and becomes depleted in younger sediments. The inverse correlation of TOC and $CaCO_3$ may be related to a change in the type of sediment input. During glacial periods, intensified upwelling may be responsible for changes in the source of nutrients flowing into the euphotic zone, thereby altering the inventory of primary producers being deposited in the sediments.

Erosion and remobilization of exposed shelf materials during glacial maxima has caused significant additional organic carbon-rich contribution to the Namibian continental slope depocenter (Summerhayes et al., 1995; Mollenhauer et al., 2002; Inthorn et al., 2006). During the LGM the sea level dropped by about 120 meters, thereby exposing the shelf depocenter and allowing eroded diatomaceous materials to be relocated to the continental slope (see Sediment Color Scans, Appendix A.) (Bard et al., 1990; Inthorn et al., 2006; Mollenhauer et al., 2002).

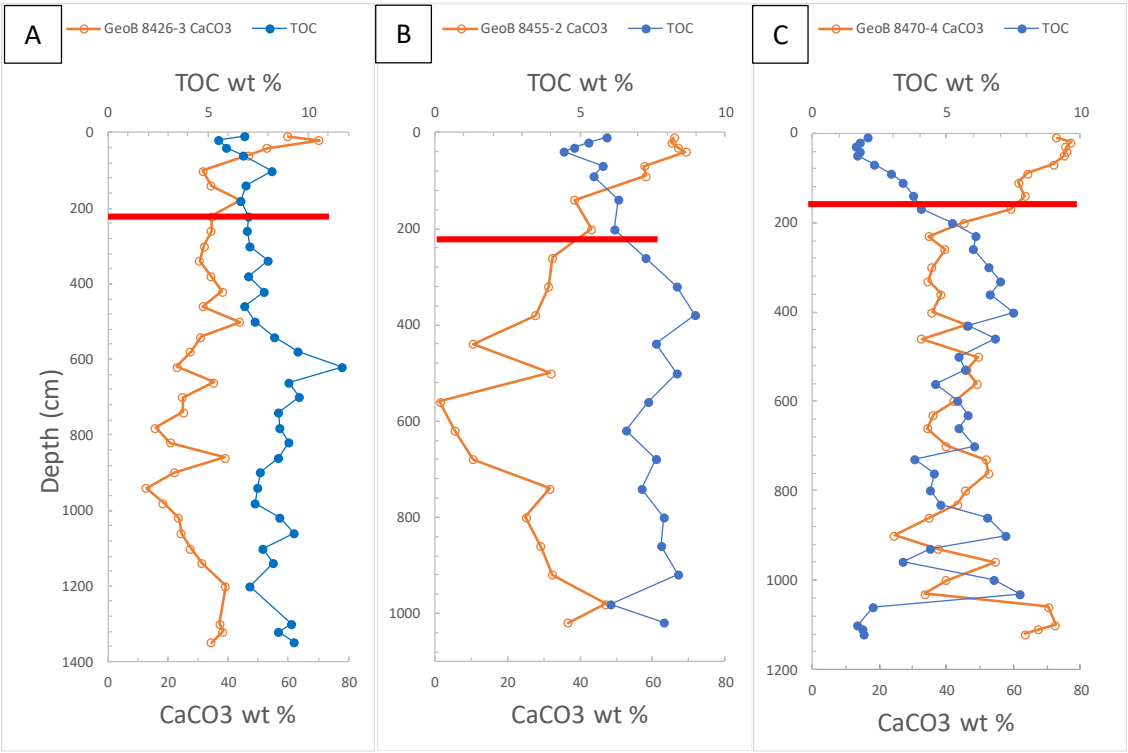

Figure 6. TOC, $CaCO_3$ profiles with LGM located. Total organic carbon (TOC) and calcium carbonate ($CaCO_3$) profiles for cores GeoB 8426-3 (A), GeoB 8455-2 (B), and GeoB 8470-4 (C). Red lines indicate the location of the LGM time slice in each core.

Analyses of phytoplankton-derived alkenones and other biogenic sediments using ^{14}C dating showed that sediments increase in age with distance from shore, indicating that sediments were initially deposited closer to shore and then transported and redeposited downslope (Mollenhauer et al., 2007).

This study considers the importance of the lateral transport system in the context of trace and major metal redox and productivity proxies. These proxies identify changes to the Benguela upwelling system that accompanied the last glacial maximum.

In order to relate productivity, sediment input type, and redeposition of shelf sediments to specific enrichments and depletions of TOC and $CaCO_3$, the profiles shown in figure 7 have been placed in the context of a time frame.

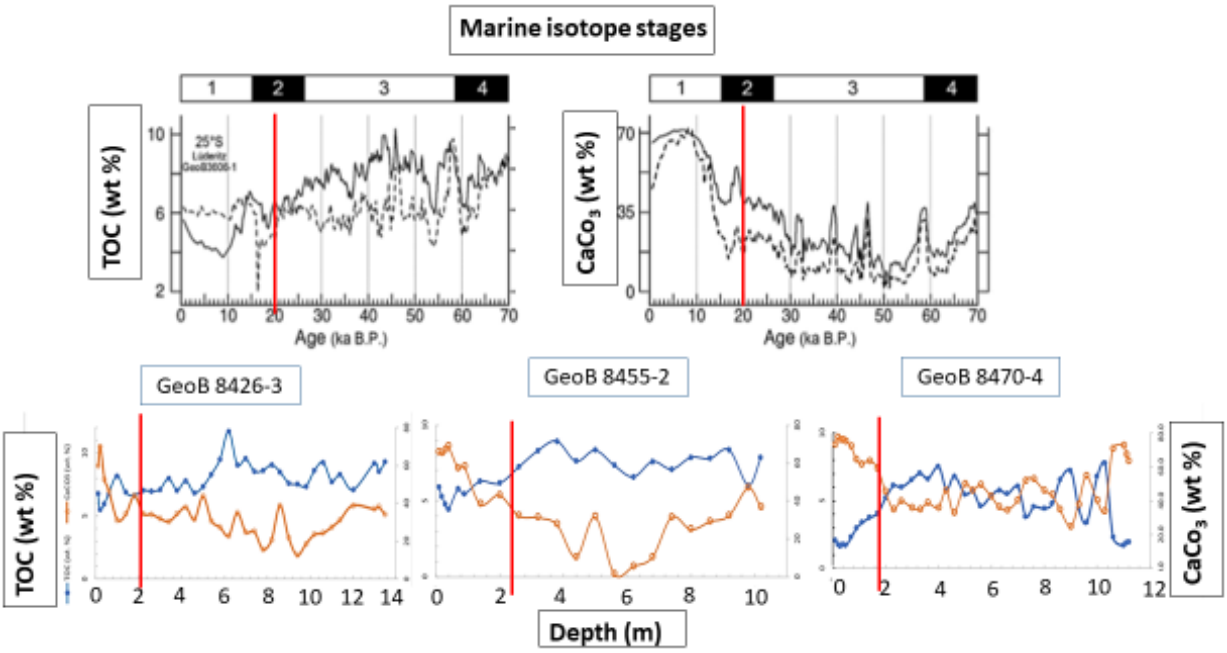

Figure 7. Correlation of Profiles of Romero et al (2010). Correlation of total organic carbon (TOC) and calcium carbonate ($CaCO_3$) profiles from cores GeoB 8426-3, GeoB 8455-2, and GeoB 8470-4 against profiles of nearby core GeoB 3606-1 from Romero et al., 2010. Red lines indicate locations of 20 ka B.P. time slice.

In order to do so, a comparison is made here with cores collected nearby and analyzed in another study. Using ^{14}C dating, Romero (2010) examined core GeoB 3606-1 (collected at 25.467ºS, 13.083ºE, in proximity to site GeoB 8455-2) and noted that sedimentation rates remain above 40 cm/ka for most of the 70 ka–year period represented by core GeoB 3606-1. However, sedimentation rates recorded in core GeoB 3606-1 in sediments younger than the LGM are much lower (approximately 22 cm/ka). Decreased sedimentation rates following the LGM may correlate to less terrigenous input, reduced primary productivity, and lower amounts of eroded shelf sediments deposited downslope. Correlation of the sediment profiles used in this study to the TOC and $CaCO_3$ profiles of core GeoB 3606-1 Romero (2010) places the LGM at approximately 220 cm in core GeoB 8426-3, 230 cm in core GeoB 8455-2, and 185 cm in the core deepest on the slope, GeoB 8470-4 (Figure 7).

All cores in this study show unexpected accumulation of high percentages of TOC prior to the LGM. High accumulation of TOC is unexpected because sediments are deposited under water columns which are at least partially oxic in the modern setting. Accumulation of TOC increases in each of the cores (Figure 6) downcore approaching the LGM. Responses of trace metals to the environmental conditions responsible for increased TOC accumulation are used in this study as tools for reconstruction of paleoredox and paleoproductivity processes in the Benguela system.

Nickel in the cores investigated in this study (Figure 8) show a strong positive linear correlation to TOC in core (GeoB 8470-4) on the lower slope, but no good overall

correlation in the profiles of the two cores from the shallower slope. A previous study indicates that Namibian mudbelt sediments show a very good correlation between nickel and TOC because nickel is stoichiometrically associated with chlorins (the degraded remains of chlorophyll pigments), and therefore directly correlative to productivity (Böning et al., 2015). The very strong correlation between nickel and TOC that exists in the deepest core (GeoB 8470-4) is not seen in the shallower cores (Figure 8), suggesting that vertically sinking fresh organic flux is the main contributor to the TOC content in core GeoB 8470-4, as opposed to TOC transported via nepheloid layers. Sediments that were previously deposited on the shelf may have been reworked and transported to the slope (Summerhayes et al., 1995; Inthorn et al., 2006; Mollenhauer et al., 2007), and deposited at the sites of cores GeoB 8426-3 and GeoB 8455-2. The TOC content of reworked sediments may have been modified by early diagenesis (bacterial degradation) in the original depositional locations. Therefore, the ratios of Ni to TOC in the sediments in cores GeoB 8426-3 and GeoB 8455-2 have likely been modified by bacterial degradation of organic matter, and do not show strong correlations. Although this process does not preclude the likelihood of organic sinking flux on the upper slope, it does explain the greatly reduced correlation between Ni and TOC in the upper slope sediments as compared to that of the lower slope.

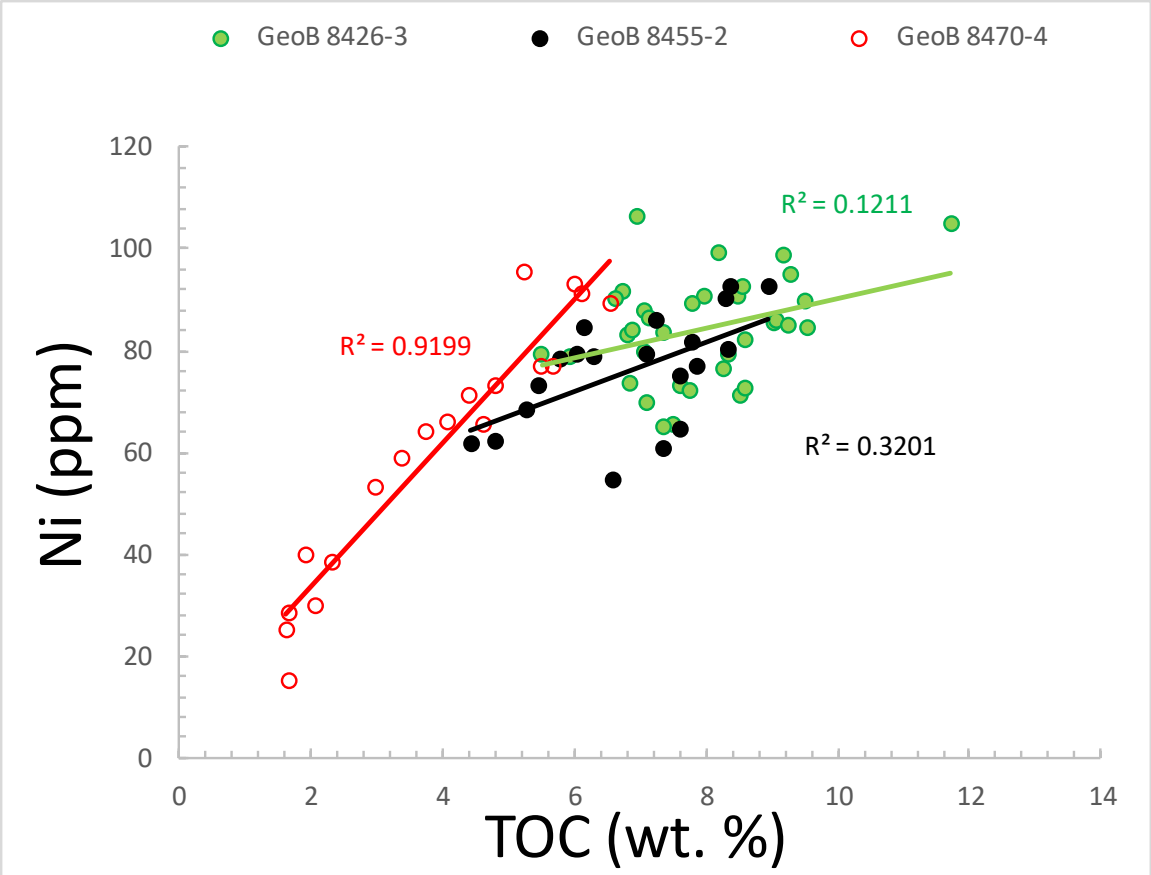

Figure 8. Ni/TOC Linear Correlation. Linear correlation of nickel (Ni) vs. total organic carbon (TOC) for cores GeoB 8426-3 (green dots), GeoB 8455-2 (black dots), and GeoB 8470-4 (red circles) with R^2 values.

Cadmium is considered an important paleoproductivity trace metal; Cd can substitute for Zn in a protein used by plankton for the assimilation of inorganic carbon from the water column (Price and Morel, 1990; Abouchami et al., 2011). Because oceanic cadmium concentrations have not changed considerably since the last glacial

maximum, cadmium profile enrichments and depletions are good indicators of changes in the supply of nutrients to a region (Boyle, 1988). In the cores used in this study, zinc and cadmium profiles follow similar paths of enrichment and depletion (Figure 9). For example, a deflection occurs at about 100 cm depth in all three cores near what may represent a period of climatic warming at the end of the Younger Dryas accompanied by a sea level rise (Walker, et al., 2009).

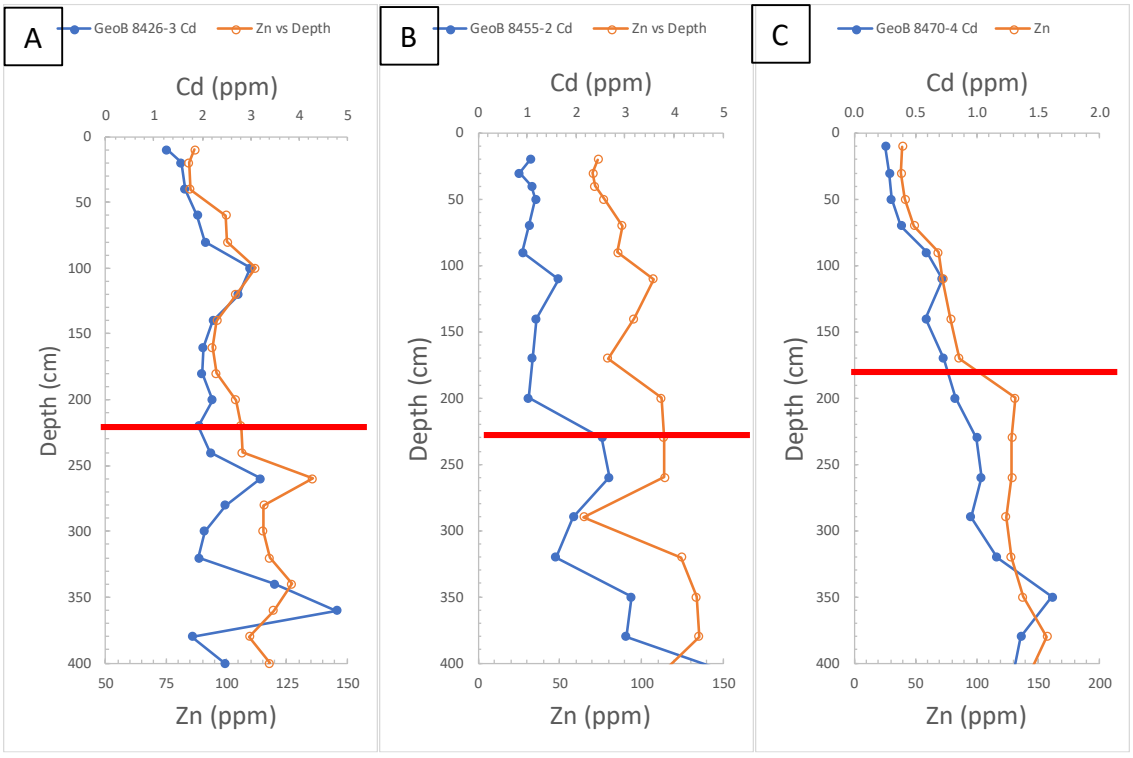

Figure 9. Cd and Zn Profiles. Cadmium (Cd) and Zinc (Zn) profiles for cores GeoB 8426-3 (A), GeoB 8455-2 (B), and GeoB 8470-4 (C). Red lines indicate the location of the 20 ka B.P. time slice.

At the LGM time slice, the zinc and cadmium profiles noticeably decouple in all cores, possibly linked to a change in the source of nutrients to the Benguela upwelling system. In the contemporary Benguela system, nutrient rich, oxygen poor South Atlantic Central Water (SACW) flows into the Benguela system from the north (Stramma and England, 1999), from which the modern upwelling is sourced. During the LGM, the upper water column may have changed such that upwelling was sourced from the Antarctic Intermediate Water – as deep as 500 m (Dingle and Nelson 1993) - influencing the availability of some nutrients. This could explain the observed changes in zinc and cadmium profiles in the cores used in this study (Figure 9). A change in nutrient supply may be an indicator of change in the geometry of the system. Upwelling from a deeper source may have occurred due to intensification of Trade Winds during glacial periods (e.g., Galbraith et al., 2004).

The Ag/V and Ag/Ni profiles show a clear correlation in all three studied cores, indicating that the productivity pathway followed by Ni and V is also followed by Ag (Figure 10). It has been shown that silver is incorporated into the siliceous shells of diatoms much more readily than into calcareous tests (Crusius et al., 2003; Flegal et al., 1995; Fisher et al., 1993), as is evident in the exceptionally low correlation between silver and calcium carbonate in all three studied cores (Figure 10). Therefore, enrichments of silver (Figure 5) may be used as a proxy for diatomaceous deposition. Depletions in silver may similarly represent decrease in diatomaceous deposition.

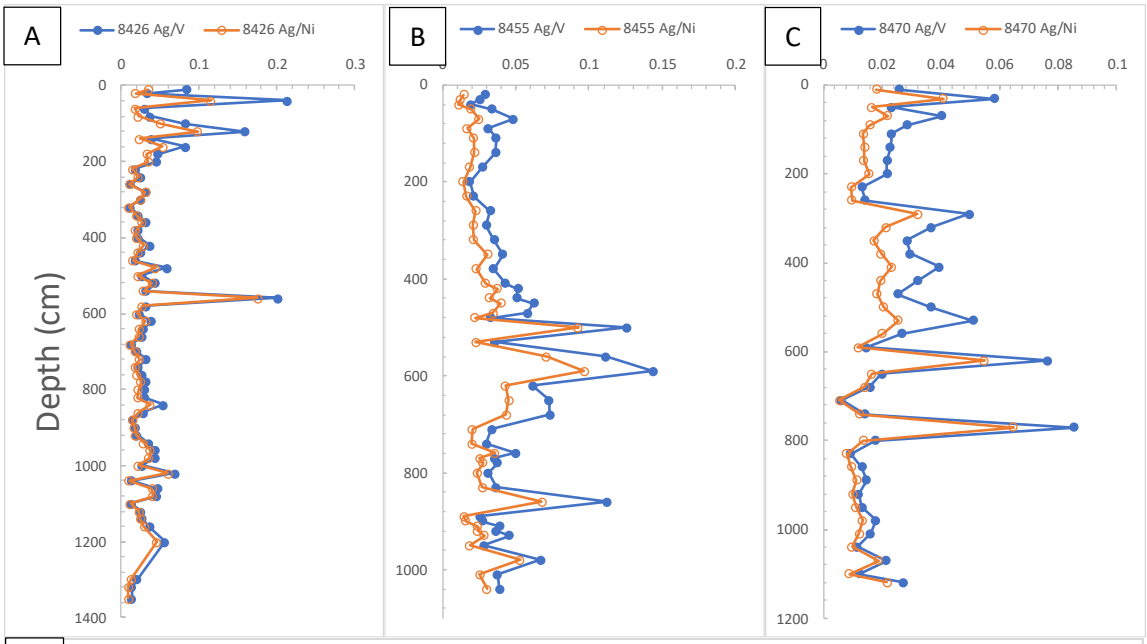
A
8426 Ag/V
8426 Ag/Ni
Depth (cm)
B
8455 Ag/V
8455 Ag/Ni
C
8470 Ag/V
8470 Ag/Ni

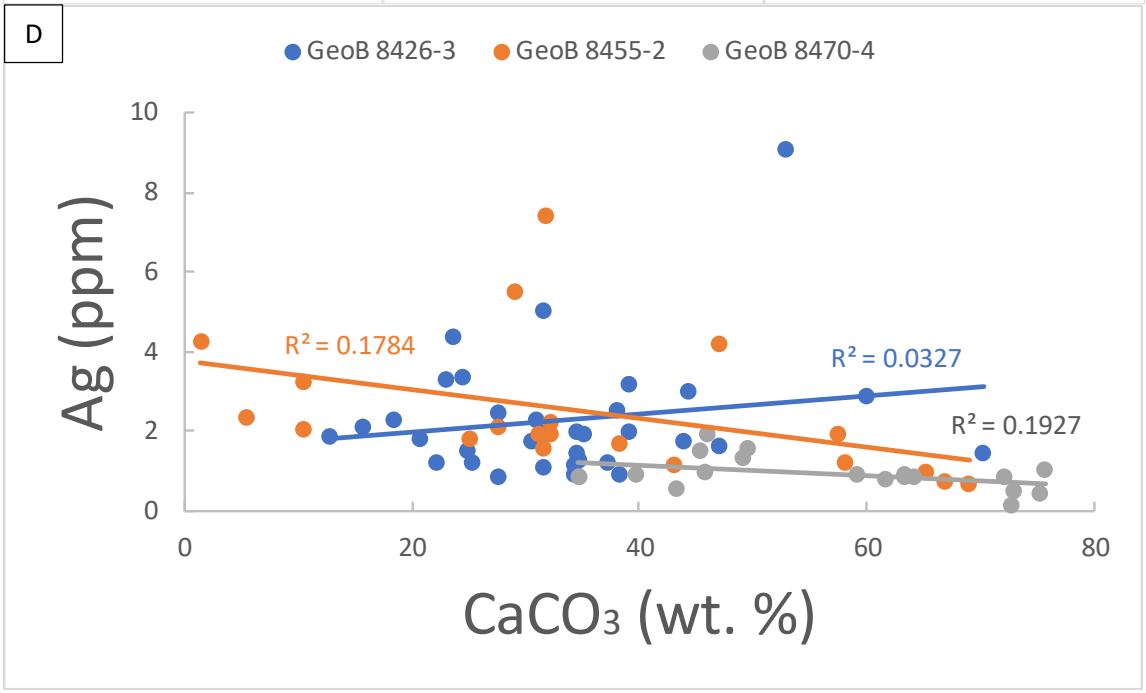
D
GeoB 8426-3
GeoB 8455-2
GeoB 8470-4
Ag (ppm)
CaCO3 (wt. %)
R² = 0.1784
R² = 0.0327
R² = 0.1927

Figure 10. (Previous page) Ag/V, Ag/Ni, and Ag to $CaCO_3$. Silver/vanadium (Ag/V) and silver/nickel (Ag/Ni) relationships for cores GeoB 8426-3 (A), GeoB 8455-2 (B), and GeoB 8470-4 (C). Linear correlation between Ag and $CaCO_3$ (calcium carbonate) for all three cores (D).

Silver contents are depleted approaching the LGM time slice in all cores, and then enriched in sediments younger than the LGM in cores GeoB 8426-3 and GeoB 8455-2. (Figure 5). The depletion in silver approaching the LGM can be correlated to drawdown in diatomaceous deposition during this time period, which is consistent with the Walvis opal paradox - decrease in diatom deposition during glacial periods (Berger and Wefer, 2002).

The previously described productivity proxies are complemented by vanadium, which can be used both as a redox proxy and as a productivity proxy. Vanadium shows strong correlation with both aluminum and iron in core GeoB 8426-3, nearest to the terrigenous source (Figure 11). This correlation may be an indication that vanadium enters the system near the coast in upwelled surface waters, and is adsorbed onto terrigenously sourced iron and manganese (oxyhydr)oxides in oxic surface water (Morford and Emerson 1999; Wehrli and Stumm, 1989; Nameroff et al., 2004). This could explain the exceptionally strong correlation with both iron and manganese observed in all three cores (Figure 11). In oxic conditions, the stable vanadate anion adsorbs to iron and manganese oxyhydroxides, which likely occurred in the oxic bottom

water. The result is high correlations between V, Fe, and Mn in all three sediment columns (Figure 11). In the lower slope core GeoB 8470-4, the high average contents of vanadium (49.86 ppm) retains very strong correlations with iron (r^2 = 0.939), manganese (r^2 = 0.915), and TOC (r^2 = 0.794). Although high concentrations of vanadium can indicate anoxic conditions in the water column, the strong correlation of V to Fe and Mn suggests oxic conditions at the sediment-water interface.

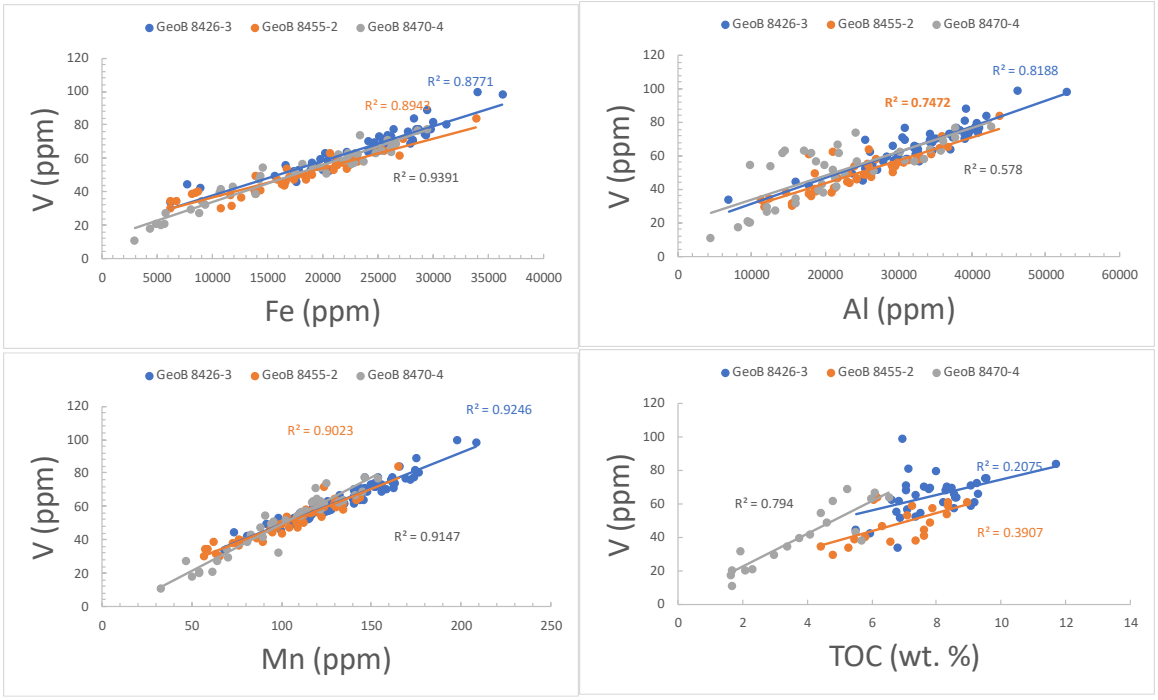

Figure 11. V/Fe, V/Al, V/Mn, and V/TOC. Linear correlations between vanadium (V) and iron (Fe) (A), aluminum (Al) (B), manganese (Mn) (C), and total organic carbon (TOC) (D) for cores GeoB 8426-3 (blue dots), GeoB 8455-2 (orange dots), and GeoB 8470-4 (gray dots) with R^2 values.

Therefore, high V concentrations during the LGM represent increases in productivity, and not anoxia. In the upper slope cores, there are also very high ratios of V/Fe and V/Mn (Figure 11), however, the relationship between V and TOC is greatly diminished in comparison to GeoB 8470-4 (r^2 values below 0.4 in both upper slope cores) (Figure 11). The strong correlation between V and TOC in the lower slope sediments may indicate that redeposited organic materials (previously affected by early diagenetic alteration after deposition on the shelf) do not make up a large fraction of the sediment deposits in core GeoB 8470-4, and therefore do not alter the V/TOC ratio. The lack of correlation between V and TOC in the upper slope cores suggests the opposite.

In agreement with this process, vanadium accumulation strongly correlates with nickel accumulation in core GeoB 8470-4 and GeoB 8455-2 (Figure 12). As described previously, Ni is an excellent indicator of sinking organic flux. Therefore, the strong correlation of V with Ni both on the middle and lower slope (cores GeoB 8455-2 and GeoB 8470-4) suggests that vanadium was biologically sequestered at the sea surface and remained with organic matter as it fell through the water column. The lack of correlation between V and Ni in core GeoB 8426-3 indicates that vanadium may have been more

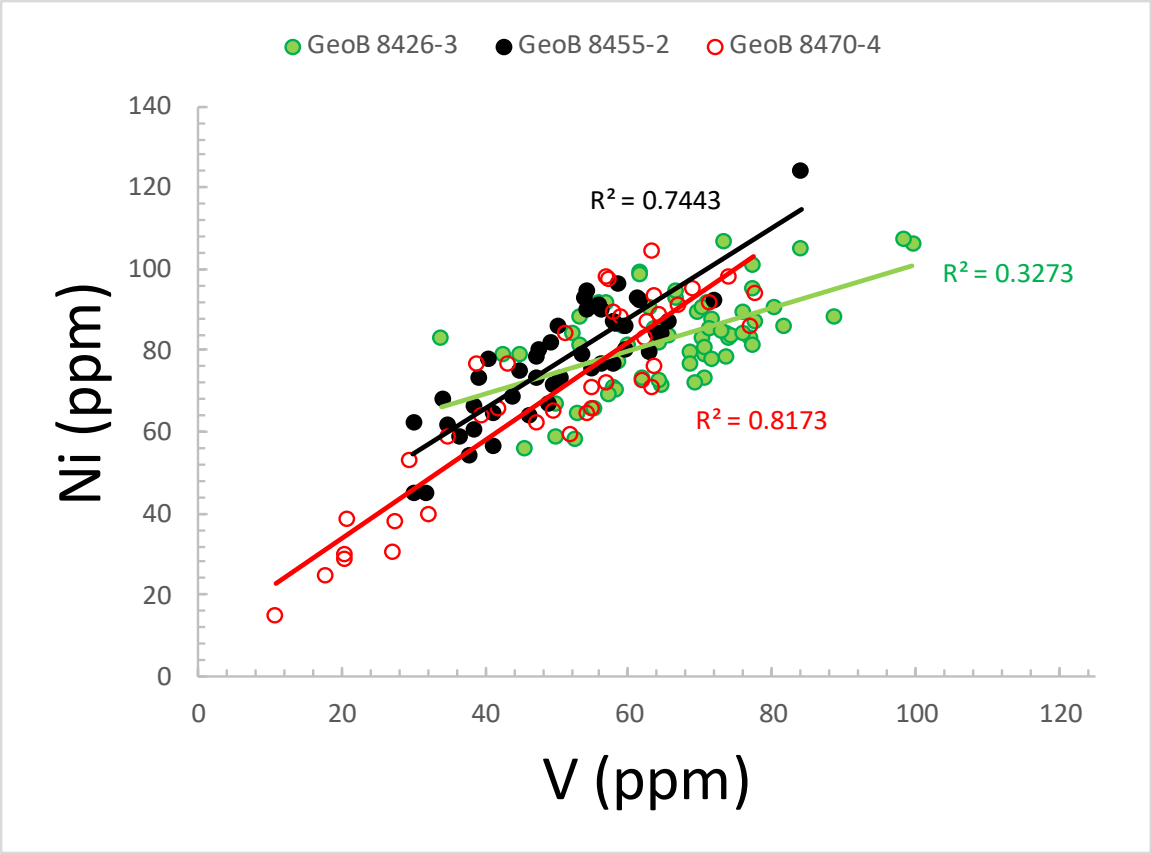

Figure 12. Ni/V. Linear correlation between nickel (Ni) and vanadium (V) for cores GeoB 8426-3 (green dots), GeoB 8455-2 (black dots), and GeoB 8470-4 (red circles) with R^2 values.

more strongly impacted by changes in redox conditions as the core of the OMZ became broader above site GeoB 8426-3 during periods of higher productivity. In euxinic water, greater accumulation of vanadium would occur in the sediments after being removed from the water column by H_2S, thereby reducing correlation between V and Ni. The other

core locations, further downslope, may not have been impacted by euxinic water conditions in the OMZ as dramatically as core GeoB 8426-3, if at all.

Using the proxies discussed here, several inferences can be made regarding depositional pathways, depositional environments, and diagenetic alterations during burial of organic carbon-rich material in the Benguela upwelling system in the time period surrounding the last glacial maximum. Oceanic carbon-rich sedimentation increased during and prior to the LGM for two reasons: increased vertical deposition due to increased primary productivity, and increased lateral transport in the bottom nepheloid layer during the oceanic lowstand. A change in the nutrient source would have impacted primary productivity, and is evident from decoupled Cd and Zn profiles and Ag depletions around the LGM. Lateral transport of materials from the shelf is evident from the lack of correlation of Ni to TOC and V to TOC and Ni to V in upper slope cores, but strong correlation in the lower slope sediments. The strong correlation of V to Mn, and V to Fe in all cores demonstrates oxic water column conditions in the bottom water at all core sites through much of the recorded time period.

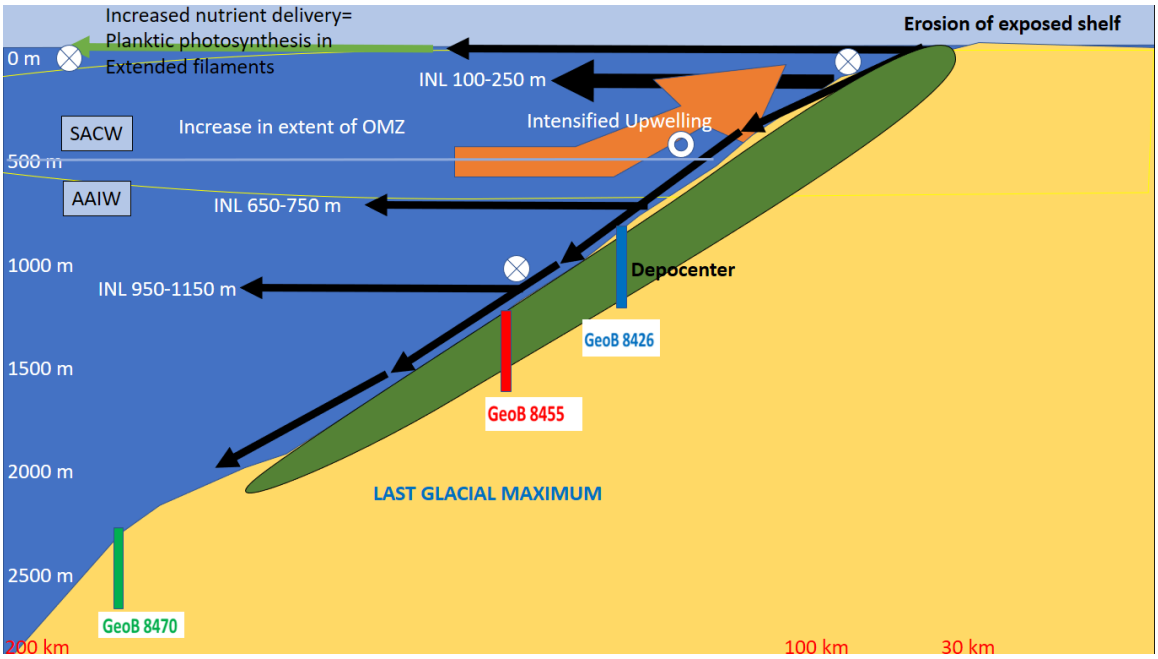

Figure 13. Proposed geometry of Benguela upwelling system during the Last Glacial Maximum (19-23 ka B.P.). Black arrows indicate OM transport in nepheloid layers. White rings indicate poleward flowing currents, and circles with an X indicate equatorward flowing currents. SACW = South Atlantic Central Water; AAIW = Antarctic Intermediate Water.

CHAPTER V

SUMMARY AND CONCLUSIONS

Good correlation of Nickel and TOC in lower slope sediments ($r^2 = 0.92$), indicates that primary productivity has been preserved well in the sediment column. Because the water column above the lower slope sediment core (GeoB 8470-4) in the modern setting is deep (2470 m) and oxic (approx. 200 μM O2 at the sediment-water interface (Inthorn et al., 2006b)), redox conditions induce remineralization of organic carbon-rich sediments in the water column. High average TOC preservation (4.58 wt. % total core) and enrichment in core GeoB 8470-4 at the LGM and in older sediments suggests that a change to anoxic conditions must have occurred in the water column above this depositional location for much of the recorded time period in cores used in this study. The lack of correlation in the Ni-TOC relationship in cores GeoB 8426-3 and GeoB 8455-2 can be connected to incorporation of shelf materials which have undergone early diagenesis. Therefore, lateral transport of shelf sediments to the upper slope sites have augmented the Ni-TOC relationship, and removed the correlation.

The V-TOC correlation in the lower slope core (GeoB 8470-4) and lack thereof in the upper slope cores (GeoB 8455-2 and GeoB 8426-3) is in agreement with the relationships between Ni and TOC in all cores; it suggests that some of the TOC in the upper slope sediments must have been influenced by processes that did not affect the

lower slope. It seems likely that additional organic matter from another source (the shelf), with a different V-TOC signal, mixed with upper slope sediments during periods when shelf sediments were reworked and transported to the upper slope. These relationships also indicate that little sediment transport and redeposition occurred as far as the lower slope core site.

The oceanic cadmium reservoir has not varied much since the last glacial maximum. Therefore, cadmium enrichments and depletions in the cores used in this study may signify changes in the nutrient supply to the Benguela upwelling system during the LGM. Cadmium profiles decouple from Zn profiles at the last glacial maximum, indicating that one metal is being used by organisms more and the other less (Cd and Zn can substitute for each other in important biological processes). This decoupling may represent a change in nutrient source in the region. Such a change could be caused by sea level fall during, for example, the last glacial maximum. Intensified upwelling may have drawn a different supply of nutrients from Antarctic Intermediate Water as opposed to the South Atlantic Central Water source in place in the modern system. A sustained record of differences in nutrient supply can be important for understanding the geometry of the system and the biological inventory likely to be deposited during isolated time slices.

Silver correlates with diatomaceous deposition in the Benguela upwelling system. Reduced diatom deposition occurs - signaled by reduced Ag concentrations - when a change in nutrients may have impacted the biological inventory of the system. The silver

proxy used in this study agrees with the cadmium proxy that a shift in the nutrient source occurred during the LGM.

Strong correlation of V, Mn, and Fe in sediments may indicate that oxic conditions have occurred at the sediment-water interface over much of the recorded time period.

Strong correlation between V and Ni occurs in both cores GeoB 8455-2 and GeoB 8470-4. This indicates that these metals were biologically sequestered. However, the V-Ni correlation does not continue in core GeoB 8426-3. This suggests that possible euxinic conditions in the water column have had a larger impact on the oceanic vanadium reservoir above site GeoB 8426-3 as the anoxic/euxinic core of the OMZ possibly became broader during glacial periods.

Our data show that changes between glacial and interglacial times not only impact the deposition of organic matter on continental margins, but also strongly influence the trace metal distribution in these sediments. The good correlation between Ni and TOC, or Ag and Ni on the lower slope and the lack of correlation on the middle and upper slope impacted by redeposition provide useful indicators of specific depositional settings. Trace metals such as silver could thus be potentially valuable tools in chemostratigraphy.

REFERENCES

Abouchami, W., Galer, S. J., de Baar, H. J., Aldercamp, A. C., Middag, R., Laan, P., . . . Andreae, M. O. (2011). Modulation of the Southern Ocean cadmium isotopesignature by ocean circulation and primary productivity. *Earth and Planetary Science Letters, 305*, 83-91.

Abrantes, F. (2000). 200 000 yr diatom records from Atlantic upwelling sites reveal maximum productivity during LGM and a shift in phytoplankton community structure at 185 000 yr. *Earth and Planetary Science Letters, 176*, 7-16.

Algeo, T. J., & Lyons, T. W. (2006). Mo-total organic carbon covariation in modern anoxic marine environments: Implications for analysis of paleoredox and paleohydrographic conditions. *Paleoceanography, 21*, 1-23.

Algeo, T. J., & Maynard, J. B. (2004). Trace element behavior and redox facies in core shales of Upper Pennsylvanian Kansas-type cyclothems. *Chemical Geology, 206*, 289-319.

Allaby, M. (Ed.). (2008). *A Dictionary of Earth Sciences* (3rd ed.). Oxford: Oxford University Press.

Azetsu-Scott, K., Johnson, B., & Petrie, B. (1995). An intermittant, intermediate nepheloid layer in Emerald Basin, Scotian shelf. *Continental shelf research, 15*(2-3), 281-293.

Bailey, G. (1991). Organic Carbon Flux and Development of Oxygen Deficiency on the Modern Benguela Continental Shelf South of 28 S: Spatial and Temporal Variability. In R. Tyson, & P. T. H. (Eds.), *Modern and ancient continental shelf anoxia* (pp. 171-183). London: Geological Society Special Publication 58.

Bailey, G. W. (1991). Organic carbon flux and development of oxygen deficiency on the modern Benguela continential shelf south of 22°S: spatial and temporal variability. In R. Tyson, & T. Pearson (Eds.), *Modern and Ancient Continental Shelf Anoxia* (Vol. 58, pp. 171-183). London.

Balistrieri, L., Brewer, P. G., & Murray, J. W. (1981). Scavenging residence times of trace metals and surface chemistry of sinking particles in the deep ocean. *Deep Sea Research Part A. Oceanographic Research Papers, 28*(2), 101-121.

Bard, E., Hammelin, B., & Fairbanks, R. G. (1990). U-Th ages obtained by mass spectrometry in corals from Barbados: Sea level during the past 130,000 years. *Letters to Nature, 346*.

Bender, M. L., Fanning, K. A., Froelich, P. N., Heath, G. R., & Maynard, V. (1977). Interstitial Nitrate Profiles and Oxidation of Sedimentary Organic Matter in the Eastern Equatorial Atlantic. *Science, 198*(4317), 605-609.

Berger, W. H., & Wefer, G. (2002). On the reconstruction of upwelling history: Namibia upwelling in context. *Marine Geology, 180*, 3-28.

Bertine, K. K. (1972). The Deposition of Molybdenum in Anoxic Waters. *Marine Chemistry, 1*(1), 43-53.

Bickert, T., & Mackensen, A. (2004). Last Glacial to Holocene Changes in South Atlantic Deep Water Circulation. In G. Wefer, S. Mulitza, & V. Ratmeyer (Eds.), *The South Atlantic in the Late Quaternary: Reconstruction of Material Budgets and Current Systems* (pp. 671-693). Verlag, Berlin, Heidelberg: Springer.

Boggs Jr, S. (1995). *Principles of Sedimentology and Stratigraphy* (2nd ed.). Upper Saddle River: Prentice-Hall, Inc.

Böning, P., Brumsack, H.-J., Bottcher, M. E., Schnetger, B., Kriete, C., Kallmeyer, J., & Borchers, S. L. (2004). Geochemistry of Peruvian near-surface sediments. *Geochimica et Cosmochimica Acta, 68*, 4429-4451.

Böning, P., Shaw, T., Pahnke, K., & Brumsack, H.-J. (2015). Nickel as indicator of fresh organic matter in upwelling sediments. *Geochimica et Cosmochimica Acta, 162*, 99-108.

Borchers, S. L., Schnetger, B., Böning, P., & Brumsack, H. J. (2005). Geochemical signatures of the Namibian diatom belt: Perennial upwellin and intermittant anoxia. *Geochemistry Geophysics Geosystems*, 1-20.

Boyd, P. W., Jickells, T., S, L. C., Blain, S., Boyle, E. A., Buesseler, K. O., . . . Takeda, S. (2007). Mesoscale iron enrichment experiments 1993-2005: synthesis and future directions. *Science, 315*, 612-617.

Boyer, D., Cole, J., & Bartholomae, C. (2000). Southwestern Africa: Northern Benguela Current Region. *Marine Pollution Bulletin, 21*(1-6), 123-140.

Boyle, E. A. (1988). Cadmium: chemical tracer od deepwater paleoceanography. *Paleoceanography, 3*(4).

Bralower, T., & Thierstein, H. (1987). Organic carbon and metal accumulation in Holocene and mid-Cretaceous marine sediments: Paleoceanographic significance. In J. Brooks, & A. Fleet (Eds.), *Marine petroleum source rocks* (Vol. 26, pp. 345-369). Blackwell, Oxford: Geological Society special publication.

Bremner, J. (1980). Physical Parameters of the Diatomaceous Mudbelt off Southwest Africa . *Marine Geology, 34*, M67-M76.

Bremner, J., & Willis, J. (1993). Mineralogy and geochemistry of the clay fraction of sediments from the Namibian continental margin and the adjacent hinterland. *Marine Geology, 115*, 85-116.

Brumsack, H. J. (2006). The trace metal content of recent organic carbon-rich sediments: Implications for Cretaceous black shale formation. *Palaeogeography, Palaeoclimatology, Palaeoecology, 232*, 334-361. doi:10.1016/j.palaeo.2005.05.011

Calvert, S. E., & Pederson, T. F. (1993). Geochemistry of Recent oxic and anoxic marine sediments: Implications for the geological record. *Marine Geology, 113*, 67-88.

Calvert, S. E., & Pederson, T. F. (2007). Elemental Proxies for Pleoclimatic and Paleoceanographic Variability in Marine Sediments: Interpretation and Application. In C. Hillaire-Marcel, & A. DeVernal (Eds.), *Developments in Marine Geology: Proxies in Late Cenozoic Paleoceanography* (Vol. 1, pp. 567-644). Amsterdam: Elsevier.

Canfield, D. A., Raiswell, R., & Bottrell, S. (1992). The Reactivity of Sedimentary Iron Minerals Toward Sulfide. *American Journal of Science, 292*, 659-683.

Capone, D. G., & Hutchins, D. A. (2013). Microbial biogeochemistry of coastal upwelling regimes in a changing ocean. *Nature Geoscience*, 711-717.

Carr, M. E. (2001). Estimation of potential productivity in eastern boundary currents using remote sensing. *Deep Sea Research Part II: Topical Studies in Oceanography*, 59-80.

Chapman, P., & Shannon, L. (1985). The Benguela ecosystem Part II. Chemistry and related processes. *Oceanogr. Mar. Biol. Annu. Rev., 23*, 183-251.

Cole, D. B., Zhang, S., & Planavsky, N. J. (2017). A new estimate of detrital redox-sensitive metal concentrations and variability in fluxes to marine sediments. *Geochimica et Cosmochimica Acta, 215*, 337-353.

Collier, R. W. (1985). Molybdenum in the Northeast Pacific Ocean. *Limnology and Oceanography, 30*(6), 1351-1354.

Cruse, A. M., & Lyons, T. W. (2004). Trace metal records of regional paleoenvironmental variability in Pensylvanian (Upper Carboniferous) black shales. *Chemical Geology, 206*, 319-345.

Crusius, J., & Thomson, J. (2003). Mobility of authigenic rhenium, silver, and selenium during postdepositional oxidation in marine sediments. *Geochimica et Cosmochimica Acta, 67*(2), 265-273.

Demaison, G., & Moore, G. (1980). Anoxic environments and oil source bed genesis. *Organic Geochemistry, 2*(1), 9-31.

Deming, J., & Baross, J. (1993). *Organic Geochemistry - Principles and Applications.* New York: Plenum Press.

Des Combes, H. J., & Abelmann, A. (2007). A 350-ky radiolarian record off Luderitz, Namibia - evidence for changes in the upwelling regime. *Marine Micropaleontology, 62*, 194-210.

Diester-Haass, L., Heine, K., Rothe, P., & Schrader, H. (1988). Late Quaternary History of Continental Climate and the Benguela Current off Southwest Africa. *65*.

Diester-Haass, L., Meyers, P. A., & Rothe, P. (1986). Light-dark cycles in opal-rich sediments near the plio-pleistocene boundary, DSDP Site 532, Walvis Ridge continental terrace. *Marine Geology, 73*, 1-23.

Dingle, R. V., & Nelson, G. (2010). Sea-bottom temperature, salinity and dissolved oxygen on the continental margin off southwestern Africa. *South African Journal of Marine Science, 13*(1), 33-49.

Dittert, N. and Henrich, R., 2000. Carbonate dissolution in the South Atlantic Ocean: evidence from ultrastructure breakdown in Globigerina bulloides. Deep Sea Research Part I: Oceanographic Research Papers, 47(4), pp.603-620.

Dupont, C. L., Buck, K. N., Palenik, B., & Barbeau, K. (2010). Nickel utilization in Phytooplankton assemblagesfrom contrasting oceanic regimes. *Deep-Sea Research I, 57*, 553-566.

Embley, R. W., & Morley, J. J. (1980). Quaternary sedimentation and paleoenvironmental studies off Namibia. *Marine Geology, 36*, 183-204.

Embley, R., & Morley, J. (1980). Quaternary sedimentation and paleoenvironmental studies off Namibia (South-west Africa). *Marine Geology, 36*, 183-204.

Emerson, S. R., & Huested, S. S. (1991). Ocean anoxia and the concentrations of molybdenum and vanadium in seawater. *Marine Chemistry, 34*(3-4), 177-196.

Emerson, S., & Hedges, J. (1988). Processes Controlling the Organic Carbon Content of Open Ocean Sediments. *Paleoceanography, 3*(5), 621-634.

Fisher, N. S., & Wente, M. (1993). The release of trace elements by dying marine phytoplankton. *Deep-Sea Research I, 40*, 671-694.

Flegal, A. R., Sanudo-Wilhelmy, S. A., & Scelfo, G. M. (1995). Silver in the eastern Atlantic ocean. *Marine Chemistry*, 315-320.

Froelich, P., Klinkenhammer, G., Bender, M., Luedtke, N., Heath, G., Cullen, D., . . . Maynard, V. (1979). Early oxidation of organic matter in pelagic sediments of the eastern equatorial Atlantic: suhoxic diagenesis. *Geochimica et Cosmochimica Acta, 43*(1075), 1075-1090.

Galbraith, E.D., Kienast, M., Pedersen, T.F. and Calvert, S.E., 2004. Glacial-interglacial modulation of the marine nitrogen cycle by high-latitude O2 supply to the global thermocline. *Paleoceanography*, *19*(4).

Gardner, W., Walsh, I., & Richardson, M. (1993). Biophysical focring of particle production and distribution during a spring bloom in the North Atlantic. *Deep Sea Research Part II, 40*(1/2), 171-195.

Georgiev, S. V., Horner, T. J., Stein, H. J., Hannah, J. L., Bingen, B., & Rehkamper, M. (2015). Cadmium-isotopic evidence for Increasing Primary Productivityduring the Late Permian Anoxic Event. *Earth and Planetary Science Letters, 410*, 84-96.

Gingele, F., & Dahmke, A. (1994). Discrete barite particles and barium as tracers of paleoproductivity in South Atlantic sediments. *Paleoceanography, 9*, 151-168.

Giraudeau, J., & Rogers, J. (1994). Phytoplankton Biomass and sea-surface temperature estimates from sea-bed distribution of nannofossils and planktonic foraminifera in the Benguela upwelling system. *Micro-paleontology, 40*, 275-285.

Graf, G., & Rosenberg, R. (1997). Bioresuspension and biodeposition: A review. *Journal of Marine Systems , 11*(3-4), 269-278.

Hansen, A., Ohde, T., & Wasmund, N. (2014). Succession of Micro- and Nannoplankton Groups in ageing upwelled waters off Namibia. *Journal of Marine Systems, 140*, 130-137.

Hatfield, D. L., Lee, B. J., Price, N. M., & Stadtman, T. C. (1991). Selenocysteyl-tRNA occurs in the diatom Thalassiosiraand the ciliate Tetrahymena. *Mol. Microbiology, 5*, 1183-1186.

Heinrichs, H., Schulz-Dobrick, B., & Wedepohl, K. H. (1980). Terrestrial Geochemistry of Cd, Bi, Tl, Pb, Zn, Rb. *Geochimica et Cosmochimica Acta, 44*, 1519-1533.

Helz, G., Miller, C., Charnock, J., Mosselmans, J., Pattrick, R., Garner, C., & Vaughan, D. (1996). Mechanism of molybdenum removal from the sea and its concentration in black shales: EXAFS evidence. *Geochimica et Cosmochimica Acta*, 3631-3642.

Hensen, C., Zabel, M., & Schultz, H. N. (2006). Benthic Cycling of Oxygen, Nitrogen and Phosphorus. In H. D. Schultz, & M. Zabel (Eds.), *Marine Geochemistry* (Vol. 2). Verlag-Berlin-Heidelberg: Springer.

Hillaire-Marcel, C., & deVernal, A. (2007). Methods in Late Cenozoic Paleoceanography: Introduction. In C. Hillaire-Marcel, & A. deVernal, *Developments in Marine Geology: Proxies in Late Cenozoic Paleoceanography* (Vol. 1). Amsterdam: Elsevier.

Huerta-Diaz, M. A., & Morse, J. W. (1992). Pyritization of trace metals in anoxic marine sediments. *Geochimica et Cosmochimica Acta, 56*, 2681-2702.

Hulthe, G., Hulth, S., & Hall, P. O. (1998). Effect of oxygen on degradation rate of refractory and labile organic matter in continental margin sediments. *Geochimica et Cosmochimica Acta, 62*(8), 1319-1328.

Hutchings, L., van der Lingen, C., Shannon, L., Crawford, L., Verheye, H., Bartholomae, C., . . . Currie, J. (2009). The Benguela Current: An ecosystem of four components. *Progress in Oceanography, 83*, 15-32.

Inthorn, M., Mohrholz, V., & Zabel, M. (2006b). Nepheloid layer distribution in the Benguela upwelling area offshore Namibia. *Deep-Sea Research*, 1423-1438.

Inthorn, M., Wagner, T., Scheeder, G., & Zabel, M. (2006a). Lateral transport controls distribution, quality, and burial of organic matter along continental slopes in high-productivity areas. *Geology*, 205-208.

Jahnke, R., Reimers, C., & Craven, D. (1990). Intensification of recycling of organic matter at the sea floornear ocean margins. *Nature, 348*, 50-54.

Keil, R., Montlucon, D., Prahl, F., & Hedges, J. (1994). Sorptive preservation of labile organic matter in marine sediments. *Nature, 370*, 549-552.

Kristensen, E. (2000). Organic matter diagenesis at the oxic/anoxic interface in coastal marine sediments, with emphasis on the role of burrowing animals. *Hydrobiologica, 426*, 1-24.

Langmuir, D. (1978). Uranium solution-mineral equilibria at low temperatures with applications to sedimentary ore deposits. *Geochimica et Cosmochimica Acta, 42*, 547-569.

Little, S. H., Vance, D., Lyons, T. W., & McManus, J. (2015). Controls on trace metal authigenic enrichment in reducing sediments: insights from modern oxygen-deficient settings. *American Journal of Science, 315*, 77-119.

Little, S. H., Vance, D., Lyons, T. W., & McManus, J. (2015). Controls on Trace Metal Authigenic Enrichment in Reducing Sediments: Insights from Modern Oxygen-Deficient Settings. *American Journal of Science, 315*, 77-119.

Lutjeharms, J. (1996). The Exchange of Water Between the South Indian and South Atlantic Oceans. In *The South Atlantic* (pp. 125-162). Heidelberg: Springer.

Lutjeharms, J., & Meeuwis, J. (1987). The extent and variability of South-East Atlantic Upwelling. *South African Journal of Marine Science, 5*(1), 51-62.

Lutjeharms, J., & Stockton, P. (1987). Kinematics of the upwelling front off southern Africa. *South African Journal of Marine Science, 5*(1), 35-49.

Lutjeharms, J., Shillington, F., & Duncomb Rae, C. (1991). Observations of Extreme Upwelling Filaments in the Southeast Atlantic Ocean. *Science, 53*, 774-776.

Lyons, T. W., Anbar, A. D., Severmann, S., Scott, C., & Gill, B. C. (2009). Tracking Euxinia in the Ancient Ocean: A Multiproxy Perspective and Proterozoic Case Study. *Annual Review of Earth and Planetary Sciences, 37*, 507-534.

Marchesiello, P., & Estrade, P. (2009). Eddy activity and mixing in upwelling systems: a comparative. *International Journal of Earth Science, 98*, 299-308.

Martin, J. H., & Fitzwater, S. E. (1988). Iron deficiency limits phytoplankton growth in the north-east Pacific subarctic. *Nature, 331*, 341-343.

Martin, J. H., Knauer, G. A., & Gordon, R. M. (1983). Silver distribution and fluxes in northeast Pacific waters. *Nature, 305*, 306-309.

Martineza, P., Bertranda, P., Shimmieldb, G. B., Cochranea, K., Jorissena, F. J., Fosterb, J., & Dignana, M. (1999). Upwelling intensity and ocean productivity changes off Cape Blanc (northwest Africa) during the last 70,000 years: geochemical and micropalaeontological evidence. *Marine Geology, 158*(1-4), 57-74.

Marz, C., Poulton, S., Beckman, B., Kuster, K., Wagner, T., & Kasten, S. (2008). Redox sensitivity of P cycling during marine black shale formation: Dynamics of sulfidic and anoxic, non-sulfidic bottom waters. *Geochimica et Cosmochimica Acta*, 3703-3717.

McCall, G., LeMaitre, R., Malahoff, A., Robinson, G., & Stephenson, P. (1969). The Geology and Geophysics of the Ambrym Caldera, New Hebrides. *Symposium Volcanoes and Their Roots, Oxford, England*, 682-696.

McCave, I. N. (2007). Deep-Sea Sediment Deposits and Properties Controlled by Currents. In C. Hillaire-Marcel, & A. DeVernal (Eds.), *Developments in Marine Geology: Proxies in Late Cenozoic Paleoceanography* (Vol. 1). Amsterdam: Elsevier.

McKay, J. L., & Pederson, T. F. (2000). Geochemical behavior of redox-sensitive trace metals in iron-sulfide layers. *EOS, 81*, F613.

McManus, J., Berelson, W. M., Severmann, S., Poulson, R. L., Hammond, D. E., & Holm, C. (2006). Molybdenum and Uranium Geochemistry in Continental Margin Sediments: Paleoproxy Potential. *Geochimica et Cosmochimica Acta, 70*, 4643-4662.

Millero, F. J., Sotolongo, S., & Izaguirre, M. (1987). The oxidation kinetics of Fe(II) in seawater. *Geochimica et Cosmochimica Acta, 51*, 793-801.

Mix, A. C., Morey, A. E., & Pisias, N. G. (1999). Foraminiferal faunal estimates of paleotemperature: Circumventing the no-analog problem yields cool ice age tropics. *Paleoceanography, 14*(3), 350-359.

Mollenhauer, G., Schneider, R. R., Muller, P. J., Spiess, V., & Wefer, G. (2002). Glacial/Interglacial variability in the Benguela upwelling system: Spatial distribution and budgets of organic carbon accumulation. *Global Biogeochemical Cycles, 16*(4), 1-15.

Morel, F. M., Hudson, R. J., & Price, N. M. (1991). Limitation of productivity by trace metals in the sea. *36*(8), 1742-1755.

Morford, J. L., & Emerson, S. (1999). The geochemistry of redox sensitive trace metals in sediments. *Geochimica et Cosmochimica Acta, 63*(11-12), 1735-1750.

Nemeth, K., & Cronin, S. (2007). Syn- and post- eruptive erosion, gully formation, and morphological evolution of a tephra ring in tropical climate erupted in 1913 in West Ambrym, Vanuatu. *Geomorphology, 86*, 115-130. doi:10.1016/j.geomorph.2006.08.016

Pailler, D., Bard, E., Rostek, F., Zheng, Y., Mortlock, R., & Van Geen, A. (2002). Burial of redox-sensitive metals and organic matter in the equatorial Indian Ocean linked to precession. *Geochimica et Cosmochimica Acta, 66*(5), 849–865.

Pancost, R. D., Coleman, J. M., Love, G. D., Chatzi, A., Bouloubassi, I., & Snape, C. A. (2008). Kerogen-bound glycerol dialkyl tetraether lipids released by hydropyrolysis of marine sediments: A bias against incorporation of sedimentary organisms? *Organic Geochemistry, 39*(9), 1359-1371.

Pederson, T., & Calvert, S. (1990). Anoxia vs. Productivity: What Controls the Formation of Organic-Carbon-Rich Sediments and Sedimentary Rocks? *AAPG Bulletin, 74*(4), 454-466.

Price, N. M., & Morel, F. M. (1990). Cadmium and cobalt substitution for zinc in a marine diatom. *Nature, 344*, 658-660.

Radebaugh, J., Lopes, R. M., Howell, R. R., Lorenz, R. D., & Turtle, E. P. (2016). Eruptive behavior of the Marum/Mbwelesu lava lake, Vanuatu and comparisons with lava lakes on Earth and Io. *Journal of Volcanology and Geothermal Research, 322*, 105-118.

Riedinger, N., Kasten, S., Groger, J., Franke, C., & Pfeifer, K. (2006). Active and buried authigenic barite fronts in sediments from the Eastern Cape Basin. *Earth and Planetary Science Letters, 241*, 876-887.

Robbins, L. J., Lalonde, S. V., Planavsky, N. J., Partin, C. A., Reinhard, C. T., Kendall, B., . . . Poulton, S. (2016). Trace Elements at the Intersection of Marine Biological and Geochemical Evolution. *Earth Science Reviews, 163*, 323-348.

Robin, C., Eissen, J.-P., & Monzier, M. (1993). Giant tuff cone and 12-km-wide associated caldera at Ambrym Volcano (Vanuatu, New Hebrides Arc). *Journal of Volcanology and Geothermal Research, 55*, 225-238. doi:0377-0273/93

Robinson, R., Meyers, P., & Murray, R. (2002). Geochemical evidence for variations in delivery and deposition of sediment in Pleistocene light-dark color cycles under the Benguela Current Upwelling System. *Marine Geology, 180*(1), 249-270.

Rogers, J., & Bremner, J. (1991). The Benguela Ecosystem: Part VII. Marine geological aspects. *Oceanography and Marine Biology - An Annual Review, 29*, 1-85.

Romero, O. E. (2010). Changes in Style and Intensity ofproduction in the Southeastern Atlantic over the last 70,000 years. *Marine Micropaleontology, 74*, 15-28.

Rosenthal, Y., Lam, P., & Boyle, E. A. (1995). Authigenic cadmium enrichments in suboxic sediments: Precipitation and postdepositional remobilization. *Earth and Planetary Science Letters, 132*, 99-111.

Rullkötter, J. (2006). Organic Matter: The Driving Force for Early Diagenesis. In H. D. Schultz, & M. Zabel (Eds.), *Marine Geochemistry* (pp. 125-168). Verlag: Springer.

Sarnthein, M., Winn, K., Duplessy, J.-C., & Fontugne, M. R. (1988). Global variations of surface ocean productivity in low and mid latitudes: Influence on CO2 reservoirs of the deep ocean and atmosphere during the last 21,000 years. *Paleoceanography, 3*, 361-399.

Schnetger, B., Brumsack, H.-J., Schale, H., Hinrichs, J., & Dittert, L. (2000). Geochemical characteristics of deep-sea sediments from the Arabian Sea: a high-resolution study. *Deep Sea Research Part II: Topical Studies in Oceanography, 47*(14), 2735-2768.

Scholz, F., McManus, J., Mix, A. C., Hensen, C., & Schneider, R. R. (2014, June). The impact of ocean deoxygenation on iron release from continental margin sediments. *Nature Geoscience, 7*, 433-437.

Scott, C., & Lyons, T. W. (2012). Contrasting molybdenum cycling and isotopic properties in euxinic versus non-euxinic sediments and sedimentary rocks: Refining the paleoproxies. *Chemical Geology, 324-325*, 19-27.

Scott, C., Planavsky, N. J., Dupont, C. L., Kendall, B., Gill, B. C., Robbins, L. J., . . . Lyons, T. W. (2013). Bioavailability of zinc in marine systems through time. *Nature Geosciences, 6*, 125-128.

Shannon, L. V. (1985). The Benguela Ecosystem Part I. Evolution of the Benguela. Physical Features and Processes. *Oceanography and Marine Biology Annual Review, 23*, 105-182.

Smillie, R. H., Hunter, K., & Loutit, M. (1981). Reduction of chromium(VI) by bacterially produced hydrogen sulphide in a marine environment. *Water Research, 15*(12).

Sorensen, J., Jorgensen, B. B., & Revsbech, N. P. (1979). A Comparison of Oxygen, Nitrate, and Sulfate Respiration in Coastal Marine Sediments. *Microbial Ecology, 5*, 105-115.

Stanley, S. M., & Luczaj, J. A. (2015). *Earth System History.* New York: W.H. Freeman and Company.

Stramma, L., & England, M. (1999, September 15). On the water masses and mean circulation of the South Atlantic Ocean. *104*(C9), 20863-20883.

Stramma, R., & Peterson, R. G. (1989). Geostrophic Transport in the Benguela Current Region. *Journal of Physical Oceanography, 19*, 1440-1448.

Suess, E., & Thiede, J. (1983). *Coastal upwelling: Its sediment record. Part A: Responses of the sedimentary regime to present coastal upwelling.* New York: Plenum Press.

Summerhayes, C., Bornhold, B., & Embley, R. (1979). Surficial Slides and slumps on the continental slope and rise off South West Africa. *Marrine Geology, 31*, 265-277.

Summerhayes, D., Kroon, D., Rosell-Mele, A., Jordan, R., Schrader, H.-J., Hearn, R., . . . Eglinton, G. (1995). Variability in the Benguela Current upwelling system over the past 70,000 years. *Progress in Oceanography, 35*, 207-251.

Tribovillard, N., Algeo, T. J., Lyons, T., & Riboulleau, A. (2006). Trace metals as Paleoredox and Paleoproductivity Proxies: An Update. *Chemical Geology, 232*, 12-32.

Volbers, A., Niebler, H.-S. G., Schmidt, H., & Henrich, R. (2004). Palaeoceanographic Changes in the Northern Benguela Upwelling System over the last 245,000 Years as Derived from Planktic Foraminifera Assemblages. In G. Wefer, S. Mulitza, & V. Ratmeyer (Eds.), *The South Atlantic in the Late Quaternary: Reconstruction of Material Budgets and Current Systems* (pp. 601-622). Berlin : Springer-Verlag .

Wakeham, S. G., & Lee, C. (1989). Organic geochemistry of particulate matter in the ocean: The role of particles in oceanic sedimentary cycles. *Organic Geochemistry, 14*(1), 83-96.

Walker, M., Johnsen, S., Olander Rasmussen, S., Popp, T., Steffensen, J.-P., Gibbard, P., Lowe, D. J. et al. (2009). Formal definition and dating of the GSSP (Global Stratotype Section and Point) for the base of the Holocene using the Greenland NGRIP ice core, and selected auxiliary records.

Wanty, R., & Goldhaber, M. (1992). Thermodynamics and kinetics of reactions involving vanadium in natural systems: Accumulation of vanadium in sedimentary rocks. *Geochimica et Cosmochimica Acta, 56*, 1471-1484.

Wefer, G., Berger, W. H., Richter, C., & al, e. (1998). *Proceedings of the Ocean Drilling Program, Initial Reports, Vol. 175, Site 1084.* Scientific Report.

Wehausen, R., & Brumsack, H.-J. (1999). Cyclic variations in the chemical composition of eastern Mediterranean Pliocene sediments: a key for understanding sapropel formation. *Marine Geology, 153*, 161-176.

Wehrli, B., & W, S. (1989). Vanadyl in natural waters: adsorption and hydrolysis promote oxygenation. *Geochimica et Cosmochimica Acta, 53*, 69-77.

Wunsch, C. (2002). What is the Thermohaline Circulation? *Science, 298*(5596).

Yao, W., & Millero, F. J. (1996). Oxidation of hydrogen sulfide by hydrous Fe(III) oxides in seawater. *Marine Chemistry, 52*.

Zabel, M., Schneider, R. R., & Bruchert, V. (2003). *METEOR-Berichte 05-1 The Benguela Upwelling System 2003 Cruise No. 57 January 20 – April 13, 2003.* Hamburg: Universität Hamburg.

APPENDICES

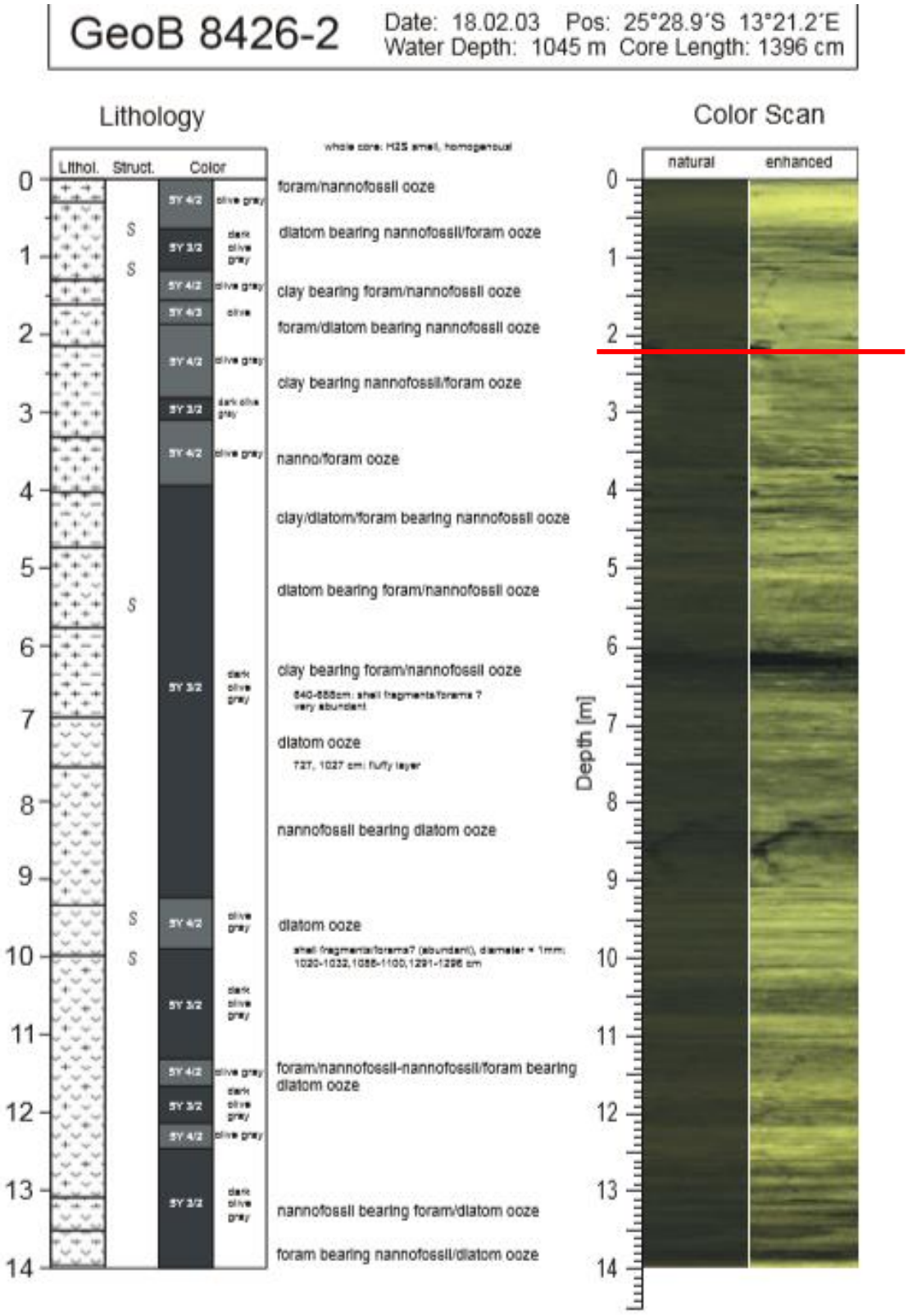
GeoB 8426-2
Date: 18.02.03 Pos: 25°28.9´S 13°21.2´E
Water Depth: 1045 m Core Length: 1396 cm
Lithology
Color Scan
Litho.
Struct.
Color
natural
enhanced
Depth [m]
whole core: H2S smell, homogenous
foram/nannofossil ooze
diatom bearing nannofossil/foram ooze
clay bearing foram/nannofossil ooze
foram/diatom bearing nannofossil ooze
clay bearing nannofossil/foram ooze
nanno/foram ooze
clay/diatom/foram bearing nannofossil ooze
diatom bearing foram/nannofossil ooze
clay bearing foram/nannofossil ooze
640-655cm: shell fragments/forams ? very abundant
diatom ooze
727, 1027 cm: fluffy layer
nannofossil bearing diatom ooze
diatom ooze
shell fragments/forams? (abundant), diameter < 1mm: 1020-1032,1088-1100,1291-1296 cm
foram/nannofossil-nannofossil/foram bearing diatom ooze
nannofossil bearing foram/diatom ooze
foram bearing nannofossil/diatom ooze

Appendix A. (Previous page) Lithology and color scan of core GeoB 8426-2. This core is parallel to core GeoB 8426-3. Red line indicates location of the LGM time slice. Taken from Zabel et al., 2003.

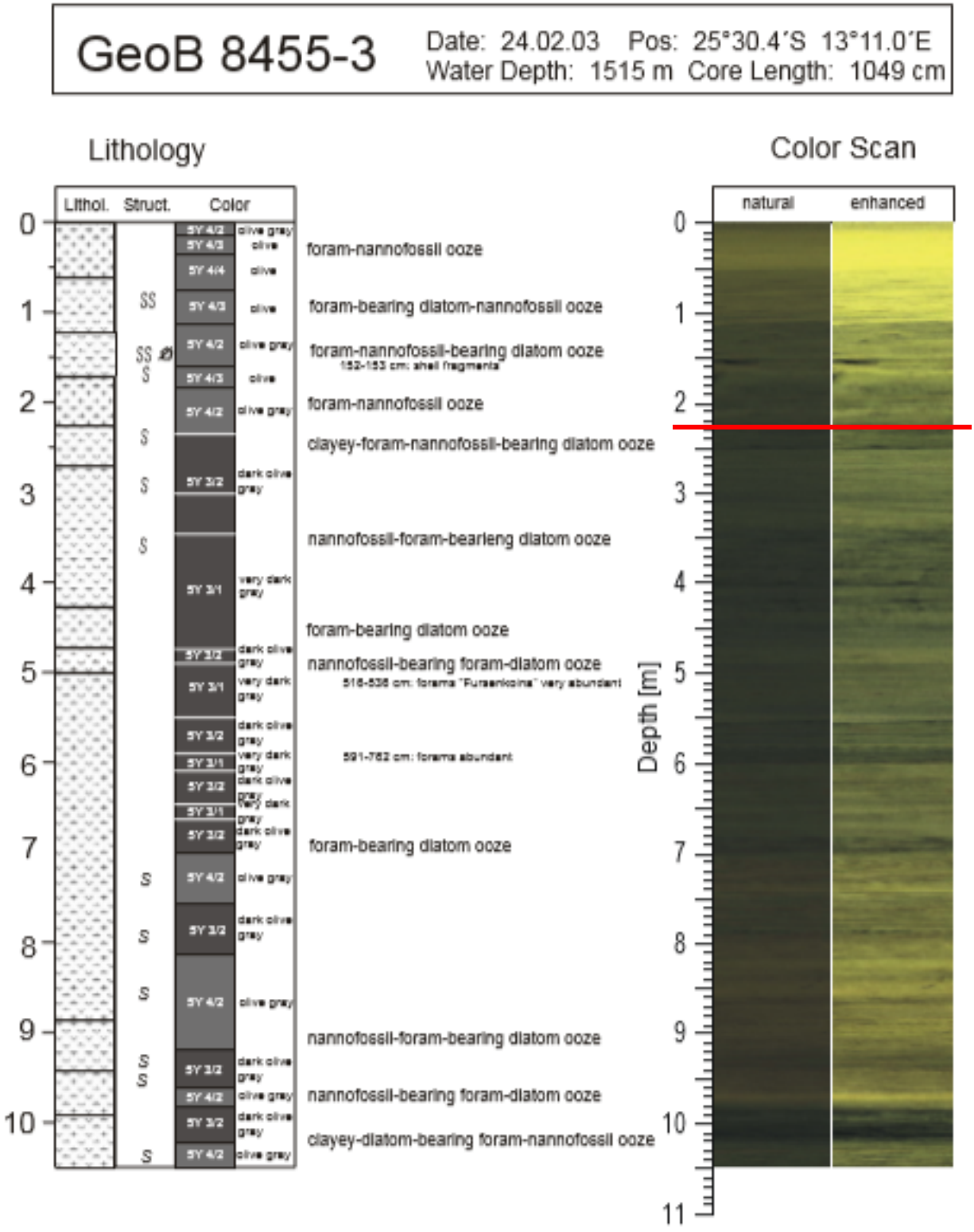

Appendix B. (Previous page) Lithology and color scan of core GeoB 8455-3. This core is parallel to core GeoB 8455-2. Red line indicates location of the LGM time slice. Taken from Zabel et al., 2003.

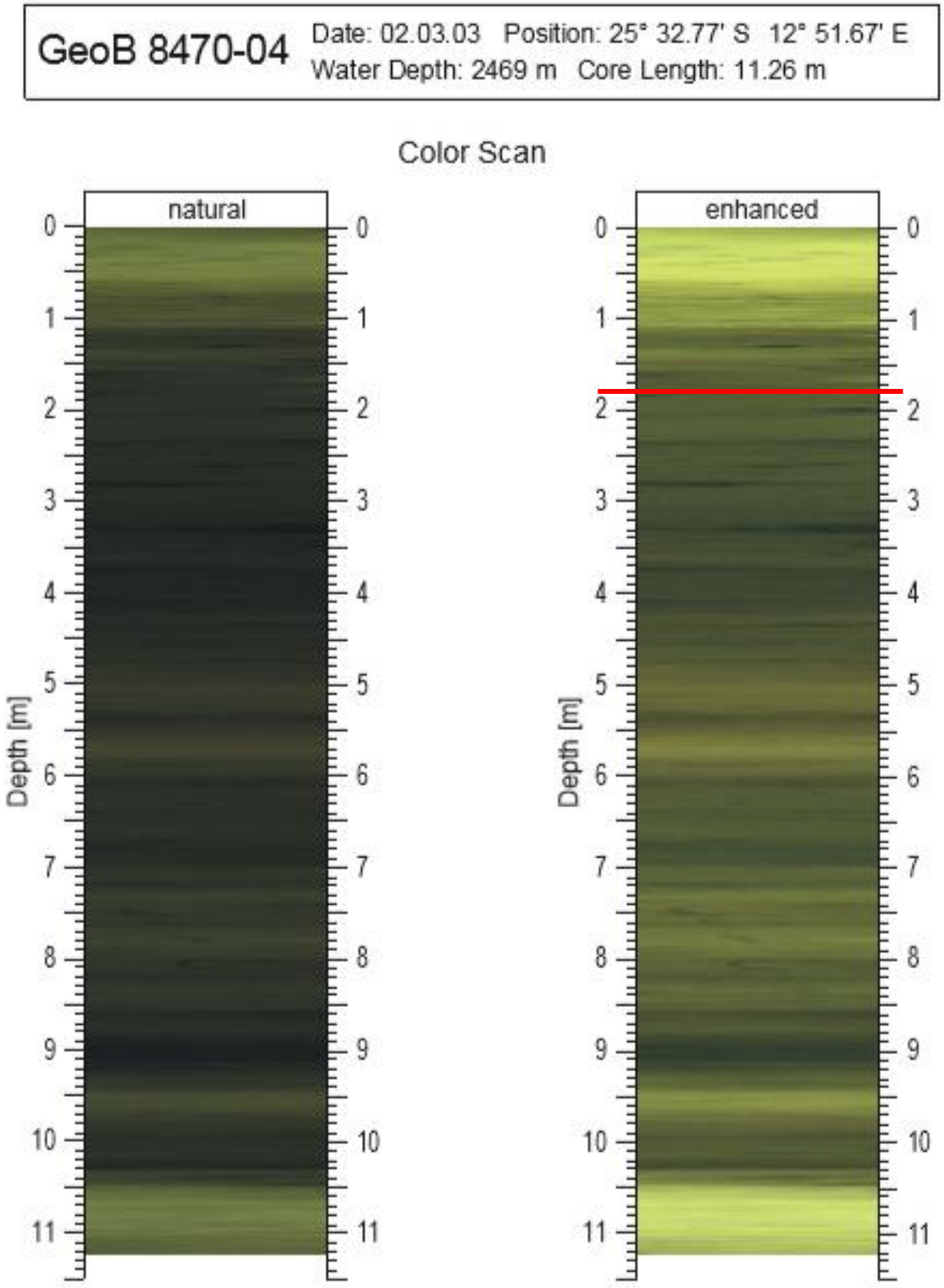

Appendix C. (Previous page) Natural and enhanced color scans of core GeoB 8470-4. Taken from Zabel et al., 2003. Red line indicates location of the LGM time slice.

VITA

Douglas William Ashe

Candidate for the Degree of

Master of Science

Thesis: TRACE METAL DISTRIBUTION IN REDEPOSITED ORGANIC CARBON-RICH SEDIMENTS IN A MODERN UPWELLING SYSTEM

Major Field: Geology

Biographical:

Education:

Completed the requirements for the Master of Science in Geology at Oklahoma State University, Stillwater, Oklahoma in July, 2018.

Completed the requirements for the Bachelor of Science in Geology at Oklahoma State University, Stillwater, Oklahoma in 2016.